Verification and Performance Analysis of Time Base Coded Data Protocol

Selva Ganesh Elangovan

A Thesis

in

The Department

of

Electrical and Computer Engineering

Presented in Partial Fulfillment of the Requirements

for the Degree of Master of Applied Science (Electrical & Computer Engineering)

at

Concordia University

Montréal, Québec, Canada

December 2012

© Selva Ganesh Elangovan, 2012

CONCORDIA UNIVERSITY

School of Graduate Studies

This is to certify that the thesis prepared

By: Selva Ganesh Elangovan

Entitled: Verification and Performance Analysis of Time Base Coded Data Protocol

and submitted in partial fulfilment of the requirements for the degree of

Master of Applied Science (Electrical & Computer Engineering)

complies with the regulations of this University and meets the accepted standards with respect to originality and quality.

Signed by the final examining committee:

_____ Dr. Rabin Raut

_____ Dr. Ibrahim Galal Hassan

_____ Dr. D. Qiu

_____ Dr. O. Ait Mohamed

Approved by _____
                            Chair of the ECE Department

_____ 2012 _____
                            Dean of Engineering

ABSTRACT

Verification and Performance Analysis of Time Base Coded Data Protocol

Selva Ganesh Elangovan

The recent improvements in implantable medical devices combined with advanced wireless sensor networks are set to revolutionize the health-care industry by providing real-time, low-cost health monitoring for the patients. A new-field called Implantable Wireless Body Sensor Networks (IWBSN) has become a hot research topic because of its energy constraints and complex design. The main components of IWBSN are the base-station and implantable sensor nodes. The most important challenge is designing the sensor nodes which has to stay inside the body for long time. A novel protocol called "Time-Based Coded Data" (TBCD) was formed in an attempt to reduce the energy consumption in the sensor nodes. While validating TBCD protocol clock drift and wireless body channel were not considered. Clock drift causes the sensor nodes to go out of synchronisation in an inconsiderable period of time. The human tissues provides a high path loss to the wireless channel. This thesis proposes an error compensation method for both delay and clock drift. This helps the base-station and sensor nodes to stay synchronised for a longer period of time. The thesis also proposes a verification framework work which focusses on providing realistic situations to validate ultra low power IWBSNs. This framework enables to prove the functionality of TBCD protocol with delay and drift calculation and enables to find the optimum transmit power, sensitivity of the transceiver for TBCD protocol to work efficiently for an optimal distance between sensor nodes and the base-station. In addition, it has been proved that the life time of the battery of sensor nodes using TBCD protocol is greater when compared to the state-of-art protocols.

ACKNOWLEDGEMENTS

TABLE OF CONTENTS

LIST OF TABLES

LIST OF FIGURES

LIST OF ACRONYMS

BAN	Body Area Networks
IWBSN	Implantable Wireless Body Sensor Networks
OSI	Open System Interconnection model
MAC	Medium Access Control
HDL	Hardware Description Language
TBCD	Time Based Coded Data
PLL	Phase Locked Loop
FSK	Frequency Shift Keying
PSK	Phase Shift Keying
ASK	Amplitude Shift Keying
OOK	On-Off Shift Keying
RTL	Register Transfer Level
MICS	Medical Implant Communication Service
ADC	Analog to Digital Converter
TDMA	Time Divison Multiple Access
FDMA	Frequency Divison Multiple Access
CSMA	Carry Sense Multiple Access/Collison Avoidence
WPAN	Wireless Personal Area Networks
PHY	Physical layer
ISM	Industrial,Scientific,Medical
GFSK	Gaussian Frequency Shift Keying
LBT	Listen before Transmit

Chapter 1

Introduction

1.1 Motivation

In 2011, an estimated 5.0 million Canadians would be 65 years of age or older and it is expected to double in the next 25 years to reach 10.4 million by 2036. An alarming prediction was made that by 2051, one in four Canadians would be over 65 years of age [7]. This increases the requirement of telemetry and also increases the cost of health-care. Body Area Networks (BAN) is one of the solution for continuous monitoring of the patients from a remote place with a reduced cost. One form of BAN is wearable biomedical health-care system. It integrates the wearable computing technology and multi-agent software architecture. Many research works were done in the field of wearable electronics such as [32, 31]. One such device is shown in Fig 1.1.

Figure 1.1: Intel "SHIMMER" sensors being worn on a patient's arm [8]

But there are some disadvantages in this form of health-care system. The wearable electronics are very uncomfortable for the patients to wear, causing an irritating skin sensation [20]. Therefore another form of BAN called Implantable Wireless Body Sensor Networks (IWBSN) is promoted widely as a future health monitoring system.

1.2 Implantable Wireless Body Sensor Networks

IWBSN comes under a unique category of BAN which enables frequent monitoring of important physiological changes such as Blood pressure, SpO2, ECG, Blood glucose etc. inside the human body. Recent advancements in the sensing technologies, Micro-electromechanical systems (MEMS) and the fusion of wireless communications have paved way for very low-cost, pervasive and ubiquitous remote health monitoring [34, 16, 29].
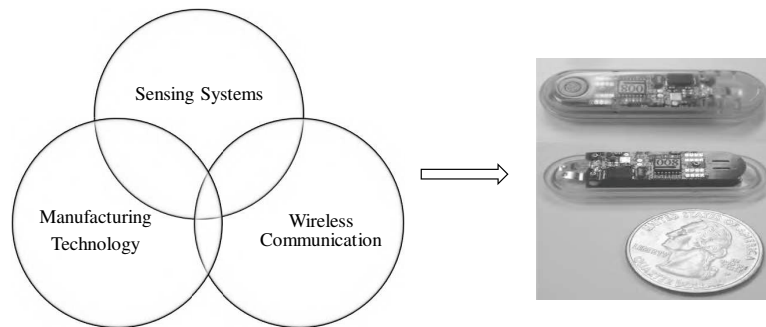
Figure 1.2: IWBSN: Fusion of technologies

This allows the patients to indulge in their daily activities without staying in hospital for many days. Meanwhile, a long-term, frequent, low-cost monitoring is made possible outside the hospital [18]. One such example of Implantable Wireless Sensor node detecting blood gases is shown in Fig 1.2 [12].

Each year, more than 30% of the one million heart attack victims in the United States die before seeking medical attention[10]. A patient always gets some

warning signs before a heart attack. IWBSN enables the patients to quickly warn the physicians when they first feel the symptoms of heart attack. Hence a long term, real-time monitoring system is highly desired by both patients and physicians.
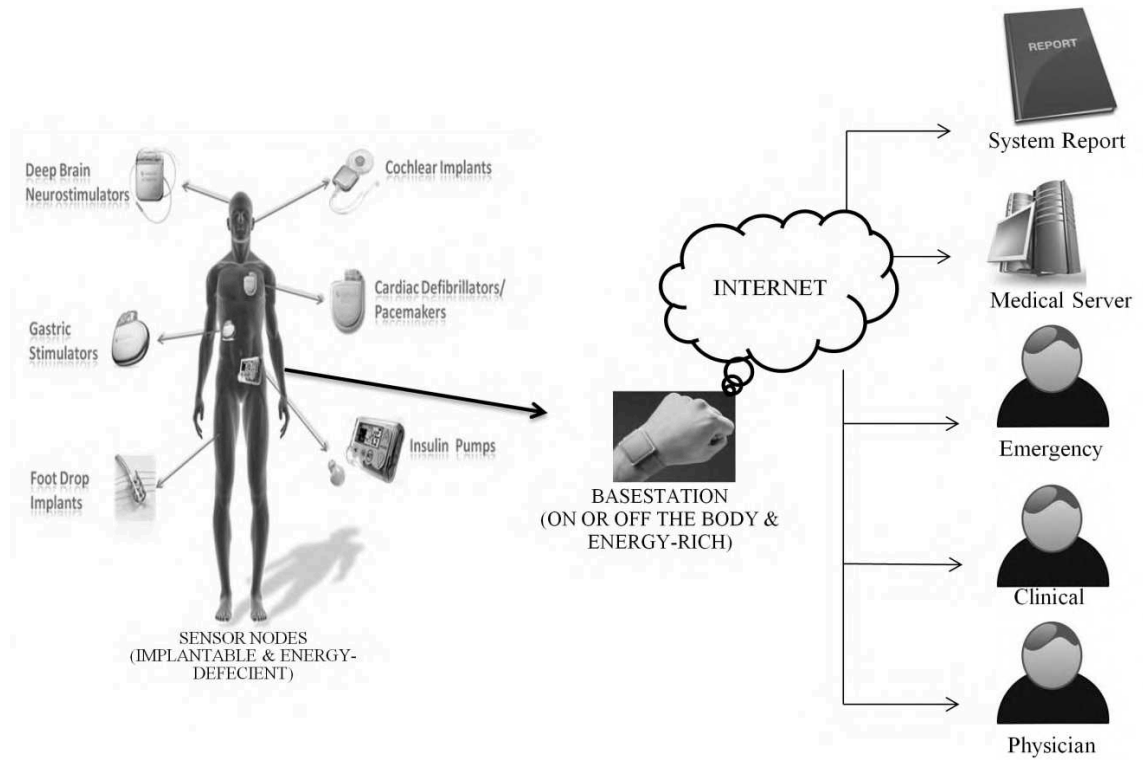
Figure 1.3: Implantable Wireless Body Sensor Networks

The Fig 1.3 shows an IWBSN with number of sensor nodes which can seamlessly integrate with the internet. Through internet, the physician could treat the patient remotely with the information obtained. But the IWBSN needs a reliable, low-power miniature and fully autonomous architecture that does not disturb the patient's activities. To design an efficient, reliable IWBSN, it is important to understand the components of IWBSNs.

1.2.1 Components of IWBSN

An IWBSN contains the following two important components:

- Base-Station on or off the body: Energy rich

- Sensor Nodes (implant devices) inside the body: Energy Deficient

The base-station is energy-rich because it is present outside the body. The power source for the base-station can be easily replaced or recharged. The sensor nodes have to stay inside the body for a long time. The body cannot be operated frequently to replace the battery of sensor node. The most important challenge in designing IWBSN is the power consumption of the sensor nodes, which has to stay inside the body for a long time. Therefore it is important to analyze the factors that make the sensor node to consume more energy [6].

The major components of the sensor node are:

- Battery

- Bio-Sensor

- Amplifier

- Analog to Digital Converter

- Logic (contains MAC protocol for the node)

- Microcontroller (for controlling the transceiver)

- Transceiver

In the above all mentioned components, transceivers consume most of the energy. Hence the transceivers must be inactive and turned ON only when it is required. There are many techniques to reduce energy consumption in the sensor node. Mostly, it is at the last two layers of the OSI model as shown in Fig.1.4:
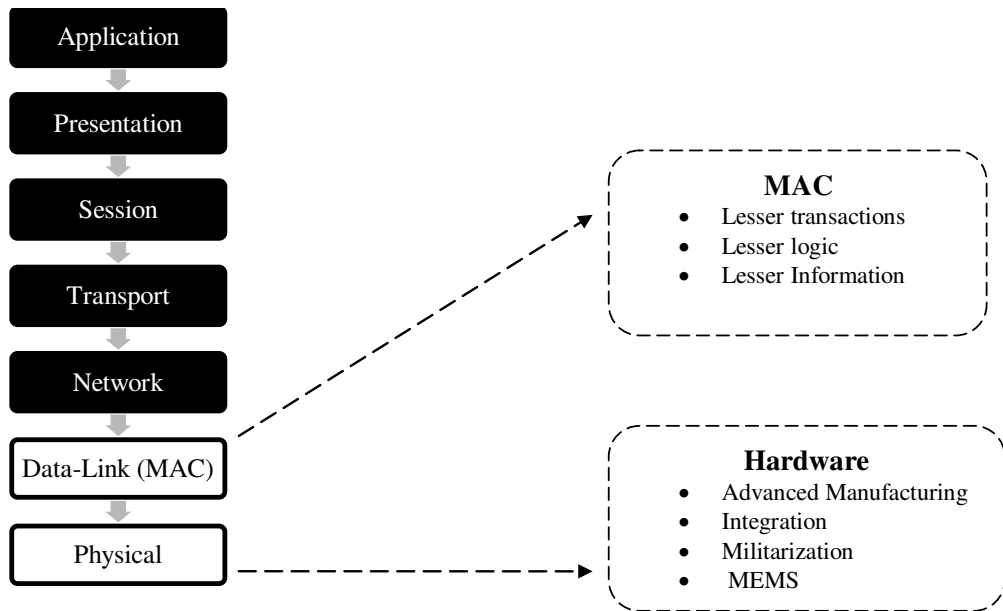
Figure 1.4: Scope in OSI layers

- By reducing the processing done in Medium Access Control (MAC) layer

- By reducing the hardware in the Physical layer

1.2.2 Medium Access Control

The scope of this thesis is in the power reduction at MAC level. The power reduction in MAC level means lesser transactions, lesser logic and transmission of lesser information. The MAC layer should be designed in a way that keeps the transceiver in sleep state always. Many attempts were made [33, 30, 11, 13, 22] to design a light weight MAC before. But all the attempts use the same standard techniques to save the energy and transmits over hundreds of control bits excluding the main data. Therefore, sensor nodes makes huge transactions even for a single byte of data.

This is a critical bottleneck in IWBSNs which keeps the transceivers in active mode for long time, killing the energy in tiny batteries within a few days or weeks.

An energy-efficient protocol called TBCD aiming to minimize the ON-time of the transceiver has been proposed in [19]. Instead of sending large number of bits for every cycle only a small time-coded data is sent wirelessly for each cycle. The use of On-Off Keying /Amplitude Shift Keying (OOK/ASK) modulation reduce the architecture complexity and power consumption by eliminating PLL, which is used widely in Frequency Shift Keying / Phase shift keying (FSK/PSK). The protocol efficiently shifts the bulk of processing to the base-station and keeps the sensors node inactive.

1.3   Thesis Contribution

This is a life-critical application and the time coded-data has to be decoded correctly in the base-station. The time coded data in TBCD protocol has to overcome two problems (i) delay between the transmitter and receiver and (ii) the environment noise [19]. Since the main theme of the protocol is the synchronization between the base-station and sensor nodes, the delay due to wireless channel is very important. Standard algorithms which tracks the synchronization is very costly in both energy and resource-wise. An algorithm for the delay calculation and error compensation in TBCD protocol was proposed in [21]. The Delay-Calculation stage would automatically calculate the delay between base-station and each sensor nodes and saves the very tiny energy present in the battery of the sensor nodes.

For TBCD protocol to work efficiently, the clocks of the base station and sensor nodes should run at the same speed. It is very important for the sensor nodes to stay synchronized in a reasonable window with the base station to avoid any significant error. But in real environment, there always occurs a phenomenon called Clock drift. Clock drift occurs when a clock does not run at the exact same speed when compared to other clocks in the network. The methodology for calculating and compensating the clock drift was not included in [21].

6

The problem of the environment noise was also unattended in the previous work. The correctness of the protocol was shown in [19] using simulations, where a wire between the sensor and base-station was considered. Though the link between the base-station and sensor node is very short, the human body presents huge path loss, requiring high transmit power or large receiver sensitivity [32]. Additionally, the signals should also overcome the interference produced by the nearby users.

Hence to verify the protocol in a practical environment, clock drift and the realistic body channel should be considered. This work is motivated to provide a realistic verification framework and to prove the ultra low power consumption of TBCD protocol.

The two main contributions of the protocols are :

- Register Transfer Level (RTL) description of base station and sensor node are provided. RTL description also includes the proposed methodology for calculating delay and clock drift of each sensor node. The clocks of the base station and sensor nodes are made to run at different speeds, to emulate a real-time environment. The compensation for clock drift is done in the sensor nodes and compensation of delay is done in the base-station.

- A performance analysis was done on TBCD protocol with a realistic body channel. Also a verification framework is proposed. This verification framework can be used to evaluate any BAN protocol and also produce a performance analysis of the protocol. This analysis gives specifications for the chip designers and enable them to produce transceivers that work efficiently and reliably in the realistic conditions.

Thus, by the above two methods, a realistic analysis results are provided for TBCD protocol.

1.4   Thesis Outline

The rest of the thesis is organized as bellow:

- Chapter 2, discusses the energy problems in the sensor nodes of BANs, provides similar MAC protocols for BANs and their disadvantages. It also presents the reason for the advent of TBCD protocol and describes it briefly. This chapter also proves that the life time of the battery (20 mAhr /3.3V Battery) of a sensor node using TBCD protocol can be prolonged to 2500 days when compared to the state-of-art ZigBee protocol.

- Chapter 3, discusses about the error created due to clock drifts in the protocol. It describes the RTL modelling and implementation in Virtex-5 FPGA of base station and sensor node with the delay, drift calculation and error compensation methodologies.

- Chapter 4, discusses the path loss due to the body fat and tissues. It presents modelling of realistic body channel in SIMULINK and verification framework in MATLAB. This framework is used for analysis of the protocol. It also presents SIMULINK modelling of base-station and sensor nodes emulating real network components.

- Chapter 5, discusses the results of verification of TBCD protocol through the methodologies discussed in Chapter 3 and 4. A performance analysis of the TBCD protocol with optimal transmit power, sensitivity for the transceivers is presented.

- Chapter 6 provides the conclusion and some future directions to the project.

Chapter 2

Medium Access Control for BAN

This chapter gives a brief introduction to the energy problems involved in designing a MAC protocol in sections 2.1 and 2.2. The similar MAC protocols for BANs and their disavantages while using in IWBSN are discussed in section 2.3. This creates a necessity for a new protocol specialised for IWBSN. The working of TBCD protocol is also discussed in section 2.4.

Implantable Wireless Body Sensor Networks (IWBSN) works in a very heterogeneous environment (i.e.) each bio-sensors inside the network are sensing different parameters which can be normal or emergency/life critical. The sensor nodes are required to transmit data at a wide range of data rates. Likewise there are many challenges imposed on the engineers while designing the components of IWBSN. Some of the key design considerations according to Common Awareness and Knowledge Platform for Studying and Enabling Independent Living (CAPSIL) [2, 14, 28, 24, 3] are given by :

- Power Consumption and Battery Life

- Protocols with huge number of transactions (wakes up the sensor nodes multiple times)

- Reliability

- Data Security and Privacy

- Biocompatibility

- RF Effects on Human Body

- Electrical Compliance

- MICS compliance

- Processing & Presentation of Data

- Body Sensor Networks Operating Systems

- Sensor Networks Development Environments

- Sensor Reporting and Maintenance

- Safety Regulations

Some of the challenges mentioned above are inversely related to each other. Some of the challenges cannot be modified because the standards are fixed. The most important challenge and that comes first is the power consumption in the sensor node.

Earlier in chapter 1, the attempts that were made to reduce the power consumption in hardware and software level were discussed briefly. The scope of this work is in software level (i.e.) reducing the activities in the MAC layer. The research goal is to preserve battery life and extend the battery replacement cycle as long as possible. The techniques that can be used to solve the above issues within MAC level are discussed in the following paragraphs. A significant research has been done on conserving the battery energy in MAC level of the sensor nodes. Hence, battery life becomes the most critical component of a sensor network. In chapter 1, the components of the sensor nodes were introduced. The total power consumption

as shown in eq(1) of the sensor node is the sum of the power consumption by the individual components.

$$P_{Total} = P_{Sensor} + P_{Amp} + P_{ADC} + P_{Logic} + P_{\mu C} + P_{Tx/Rx}(1)$$

In [20], an analysis was done using the standard components to find the component which consumes the maximum amount of energy. Table 2.1 shows the power consumption by each component of the sensor node and this better depicted in Fig 2.1. Table 2.1 and Fig 2.1 from [20] are shown here to emphasis the impact of transceivers on power consumption by the sensor node.

Table 2.1: Power Consumption by standard components [20]

	ADC/Amp [Hindawi]	Logic [RTC DS 1372]	Controller [MSP430]	Tx/Rx [ANT]
Average Power Consumption (μW)	0.3	1.2	0.3	360
Power Usage Ratio (%)	0.08	0.33	0.08	99.51
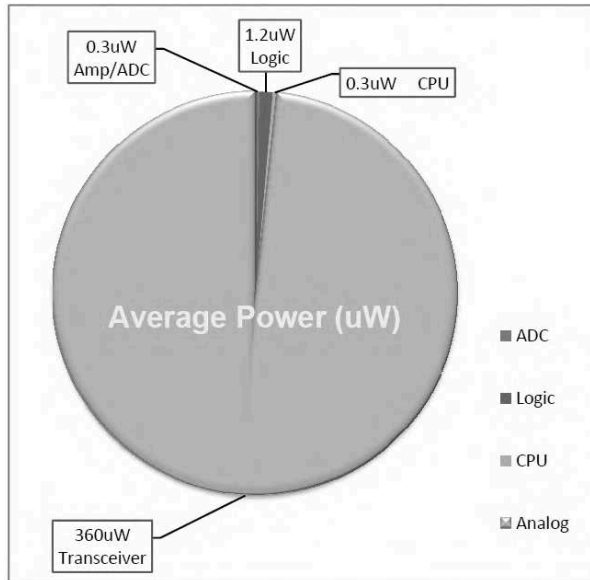
Figure 2.1: Power consumption of components of Sensor node [20]

11

In the last decade, due to Moores law, the average power consumption of wireless sensor devices has decreased greatly [2]. However similar technology growth is not found in conserving huge amount of energy in small area. Hence, computational techniques in the MAC layer is the key and some smart techniques are needed to extend the battery life.

Some of the key computational techniques used to optimize power consumption [14]:

- Low duty cycle means less ON time

- Adaptive routing algorithms

- Clock gating

- Dynamic Power Management

- Multiple sleep states

- Dynamic Voltage Scaling

- Alternative energy sources such as solar

- Power Scavenging Methods (Example: Piezoelectricity)

- Fuel cells are very promising but may not be practical at this time

The following paragraphs discuss the MAC protocols available for body sensor networks and also the common issues among those protocols.

2.1 Common protocol issues

The main design scheme of MAC protocol is discussed first before analyzing the issues in the existing protocol. The widely used techniques for MAC protocol are Time Division Multiple Access Technique (TDMA) and Carrier Sense Multiple Access Collision Avoidance (CSMA/CA). Frequency Division Multiple Access (FDMA)

needs a huge number of hardware resources resulting in high consumption of power [39]. Similarly, Code Division Multiple Access Technique (CDMA) requires complex computational techniques.

Table 2.2: Comparison between TDMA and CSMA/CA [39]

	TDMA	**CSMA/CA**
Power Consumption	Low	High
Bandwidth	Maximum	low
Traffic level (Preferred)	High	low
Dynamism (Changing Network)	Poor	Good
Synchronization	Required	May be Required

The comparison between TDMA and CSMA/CA is shown in the Table 2.2 [39]. TDMA supports the heterogeneous network because there is separate time slot for each sensor node to function. This also removes the need for constant idle listening for a clear channel as in the case of CSMA/CA technology. However TDMA requires good synchronization schemes which are difficult to implement in heterogeneous environment. Since sensor node have a constant sensing function, a simple synchronization scheme is possible. Some of the previous works in TDMA are published in [27, 26, 17]. In the following paragraphs commercially used protocol which can be used in body sensor networks are discussed.

2.2   Related works

2.2.1   IEEE 802.15.4

IEEE 802.15.4 standard for Low Data Rate (LR) Wireless Personal Area Network (WPAN) comes under the IEEE 802.15 working group which is introduced to standardize WPAN. The following diagram shows a common transaction between two nodes in the network.

Fig 2.2 shows the common transactions between two nodes in IEEE 802.15.4 protocol. Fig 2.3 shows the command frame structure of IEEE 802.15.4. The two figures are shown here to illustrate the complexity in the frame structure and how lengthy the transactions could be due to the complexity. According to Fig 2.2, for sending data each time, atleast four transactions has to take place. In addition to the original data, the control frames are attached. In each transaction, a huge frame of data is either transmitted or received. This increases the transceiver activity and in-turn consumes a large energy in tiny battery of the sensor node.
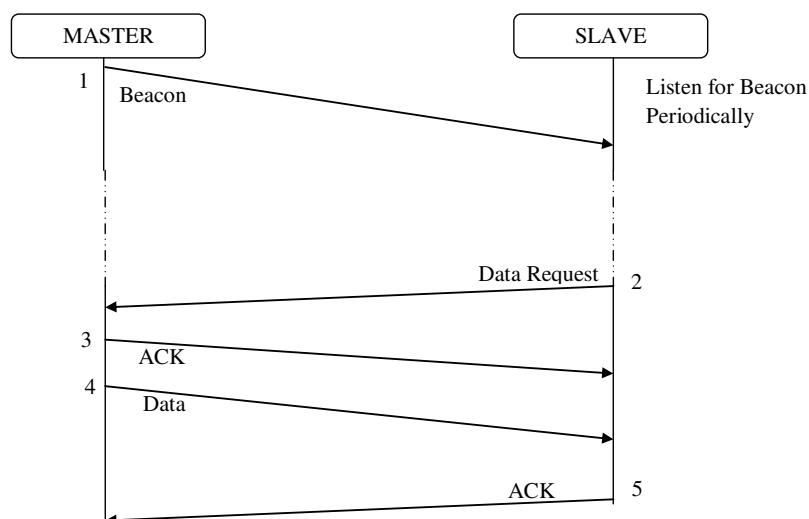
Figure 2.2: Common transactions between two nodes in IEEE 802.15.4

The MAC command frame is shown in Fig 2.3. Similarly different frames are added for various purposes. It has a MAC sub layer, PHY layer and PHY beacon packet. It carries atleast 6+(4 to 20)+n bytes of data. Most of the other BAN protocols are formed from IEEE 802.15.4. Hence they also carry different frames apart from data bits. These different frames increase the activities of the transceivers of the sensor nodes. The protocol is also very heavy in terms of the logic it carries in the nodes.

Octets	2	1	4 to 20	1	n	2
MAC sub layer	Frame Control	Sequence Number	Addressing Fields	Command Type	Command Payload	FCS
	MAC Header			MAC Service Data Unit		Footer

Octets	4	1	1	6+ 4 to 20 + n
PHY layer	Preamble Sequence	Start of Frame Delimiter	Frame Length	MAC PHY Data Unit
	Synchronization Header		PHY Header	PHY Service Data Unit
				12 + 4 to 20 + n
	PHY Beacon Packet			
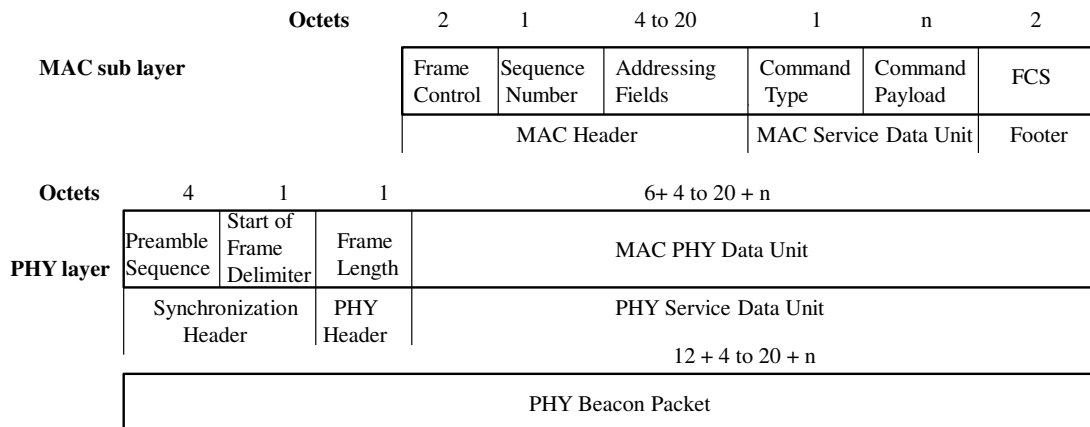
Figure 2.3: Command Frame of IEEE 802.15.4 [20]

The MAC command frame sizes are given below:

Beacon Frame size $\qquad = 13 + (4 \text{ to } 10) + k + m + n$ bytes

Data Frame size $\qquad = 11 + (4 \text{ to } 20) + n$ bytes

Acknowledgement Frame size $\quad = 11$ bytes

Hence the total frame size with all the control frames is given by

(IEEE Control bytes) $\qquad = (MAC + Beacon + Data + Acknowledgement)$

$\qquad = 17 + 15 + 11 + 16$

$\qquad = 59$ bytes

This provides an insight of how large the control information is required for data transaction in IEEE 802.15.4 group.

2.2.2 Zigbee and ANT+ protocols

Similarly there are two commercially available protocols called Zigbee and ANT protocol in the market which can be used in BAN. A comparison study has been done in [20] is shown in Table 2.3 to give an idea of how the protocols help in deriving excessive activity of the transceivers.

Table 2.3: Comparison between frame structures of three commercially available protocols [20]

	IEEE 802.15.4	Zigbee	ANT+
Bytes/Req	17+	12	10
Bytes/ACK	11	15	10
Bytes/MAC	16+	0	0
Main Data	1+(min)	5+	8
Total bytes	45+	32+	18
Total bits 1 start + 1 stop bit	495+	352+	198

2.2.3 Other related works

Recently many researches were carried out in designing protocols for WBANs. Zhurong.et.al [13] designed non-standard wireless protocol architecture using star topology with ISM band Nordic's nRF24L01 chip. The PHY data bytes for this protocol are shown in Fig 2.4 to show the length of the data frame. The disadvantage for this protocol is that it uses CSMA/CA technology which consumes high amount of energy.
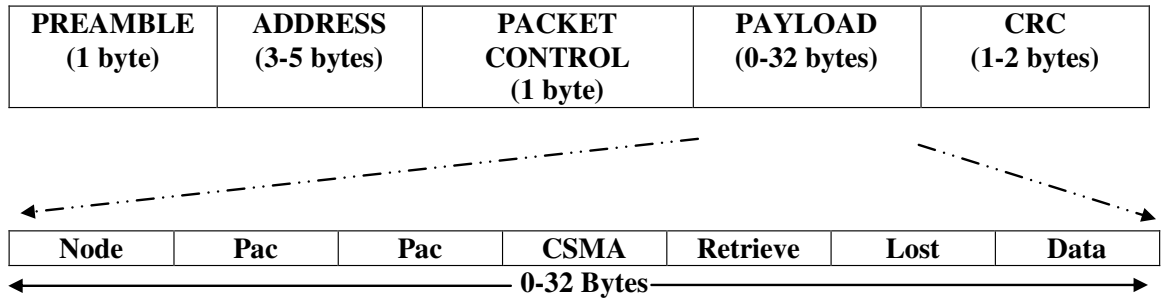
Figure 2.4: Format of PHY data unit [13]

Ameen.et.al [11] proposed a power efficient MAC protocol for implant device based on wake up table for normal communication and radio based wakeup for emergency communication. Different wake-up mechanisms for different type of traffic

16

have been proposed. The traffic is classified into normal, emergency and on-demand traffic. The main aim is to conserve significant amount of energy by using suitable wake-up mechanisms. The size of the control byte with actual data is 10 bytes. Like earlier cases, this protocol sends more control bytes, keeping the transceiver active for longer period.
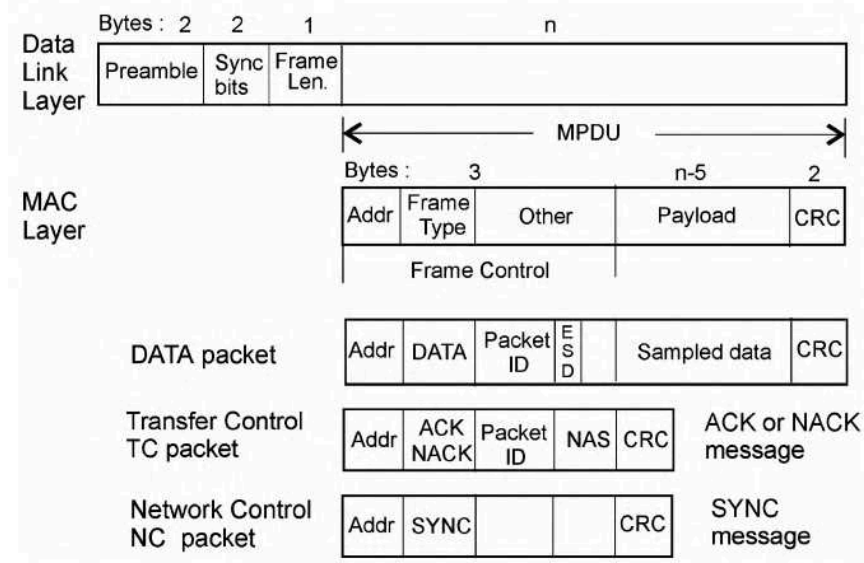
Figure 2.5: Packet format as presented in [30]

Marinkovic.et.al [30] developed an energy-efficient protocol to transfer large amount of data. A duty cycle equation was formed to predict battery life and power consumption in the sensor node. The protocol is implemented using Analog Device's ADF7020 RF transceivers employing Gaussian frequency-shift keying (GFSK) modulation. The Fig 2.5 and Table 2.4 are presented from [30] to show that the protocol makes the transceiver to stay ON for a longer period. Also GFSK technique will consume more power due to the circuit complexity.

Omeni.et.al [33] suggested an energy-efficient medium access protocol based on low power System on Chip (SOC) called $Sensium^{TM}$. A Clear Channel Assessment (CA) algorithm based on standard Listen Before Transmit (LBT) is used to avoid

Table 2.4: Frame sizes as presented in [30]

	Number of bits (Sampling rate 125 samples/sec)	Number of bits (Sampling rate 250 samples/sec)
TDMA framelength	1000	800
Overhead	80	80
ACK message	24+80	24+80
Synchronization message	80	80

any collision. A wakeup fallback time is introduced to prevent any time slot overlaps. But the $Sensium^{TM}$ architecture uses Frequency Shift keying (FSK) which increases the circuit complexity hence consuming more power.

As seen in the previous sections, one of the major problems with all other algorithms is that they use the same standard methods like TDMA or CSMA/CA and insert a lot of information with the original data. Hence to reduce the transceivers activity an efficient protocol carrying less control information is needed for IWBSN.

2.3   Time-Based Coded Data protocol

A novel protocol titled Time Based Coded Data (TBCD) protocol was formed to minimize the transceiver's activity. The solution adopted by the TBCD protocol is sending reduced number of bits for each transaction. This is done by introducing active time slots for each sensor nodes. Thus, the transceivers in the sensor nodes will be in sleep mode for longer period and wake up only for a short time in their active time slot. The protocol also calculates the propagation delay of the signals between the base station and the sensor nodes.

2.3.1 Algorithm for Base station and Sensor nodes

Earlier in chapter 1, it is discussed that the output of the Analog to Digital Converter is sent to logic block carrying Medium Access Control (MAC) of the protocol.

The algorithm for MAC for both sensor and base-station is given below.

Algorithm 1 General Algorithm for Sensor Nodes

Require: *Initialization* & *Synchronization* & *Assign Node ID*
Ensure: *Reset counters* & *Start counting ID and Data counters* $(Clk \leftarrow f\,KHz)$
  Start:
  if $ID\_Counter \leftarrow 0$ **then**
    do configuration and updates
  else
    wait *until* $ID\_Counter \leftarrow Node\_ID$ **then**
    wait *until* $Data\_Counter \leftarrow Sensor\_Data$ **then**
    Turn ON the Transmitter
    Send Short Signal
  end if
  loop Start: *repeat for the next round*
  end

Algorithm 2 General Algorithm for Base Station

Require: *Initialization* & *Synchronization* & *Assign Node ID*
Ensure: *Reset counters* & *Start counting ID and Data counters* $(Clk \leftarrow f\,KHz)$
  Start:
  if $ID\_Counter \leftarrow 0$ **then**
    wait *until the arrival of short signal* **then**
    Obtain $Sensor\_ID\,from\,ID\_Counter$
    Obtain $Sensor\_Data\,from\,Data\_Counter$
  end if
  loop Start: *repeat for the next round*
  end

As shown in the algorithm, instead of transmitting the whole sampled data from ADC in each time slot, only a pulse or a very short signal (a time coded data) will be sent by the transmitter sharply at a corresponding level to the base-station. This will keep the transceiver in sleep mode almost all the time. A brief description of TBCD protocol is given in the following paragraphs.

It is assumed that all the sensor nodes in the network went through synchronization phase and are perfectly synchronized with other sensor nodes and base-station. This is done by having the counters operating at same clock frequency and counting from the same initial value. The counters inside the sensor nodes and the base-station are split into two as shown in Fig 2.6. The lower bits of the counter is called as ID_Counter which is used to identify the time slot of a particular sensor and Data_Counter is used to identify the value of sampled level. Due to synchronization, the counters in base-station and sensors are reading the same value.

COUNTERS OF THE BASE STATION AND SENSOR NODES
(Split into two parts)

ID_COUNTER	DATA_COUNTER
(width depends on the number of sensors)	(width depends on the number of sample levels)
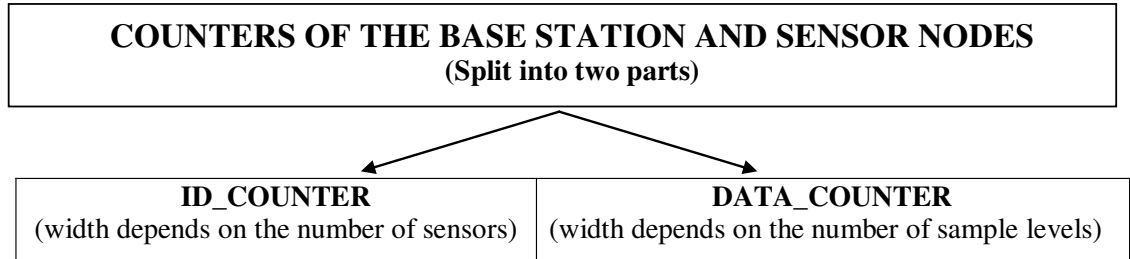
Figure 2.6: Data Counters and ID Counters of TBCD protocol

When the Data_Counter value overflows, it triggers an enable event which increments Sensor ID value. Then the Data_Counter value starts from zero, while comparator is used to compare the value of the Data_Counter and the value of sampled level. A 4 bit ID_Counter can cover up to 15 sensors. If the ID_Counter and Data_Counter values are zero, it symbolize that the sensor nodes are in initialization and configuration phase.

The transceivers on the base station are always on the body or away from the body. It can be energized periodically very easily. Hence it is not necessary for the bas station to be in sleep mode but the sensor nodes will always be kept in sleep mode except when the digitized value from ADC equals the Data_Counter value. During this event the sensor wakes up and sends a short pulse or a short signal and goes back to the sleep mode very quickly. This will help to reduce the wastage of

large amount of energy by keeping the transceiver for long time.

The base station will use their Data_Counter and ID_Counter value, when the short signal arrives to generate an address. The ADC levels are predetermined and the base station knows the range of the sampled levels. This information is stored in a look up table. The generated address is used to determine the value of bio sensed signal. Thus TBCD protocol without actually sending the whole data, informs the base-station that a particular value is sensed in a particular sensor node.

Table 2.5: Conversion table

Blood Glucose Value(mM)	ADC range
3.0	0
3.5	1
4.0	2
4.5	3
5.0	4
5.5	5
6.0	6
6.5	7

The working of TBCD protocol is shown in the Fig 2.7. Each blood glucose value is associated to one of the 3-bit binary value as shown in the Table 2.5. For example, the sensor node #1 in Figure 2.7 has read the blood glucose as 5.0mM in range [1.0,2.0,3.0,4.0,5.0,6.0,7.0,8.0] which is converted by ADC to a 3-bit binary value as 4. Whenever, the ID_Counter value matches 1 and the Data_Counter value matches 4, a short signal is sent to the base-station. The base station will receive the short signal at the instance where the ID_Counter and Data_Counter reads 1 and 4 respectively. From the Look-up table, base station will decode the actual blood glucose value 4.0. But in actual environment, there is always air delay and other environment factors that will affect the short signal. A delay calculation

21

methodology was proposed in [21] to compensate for the error due to air delay.
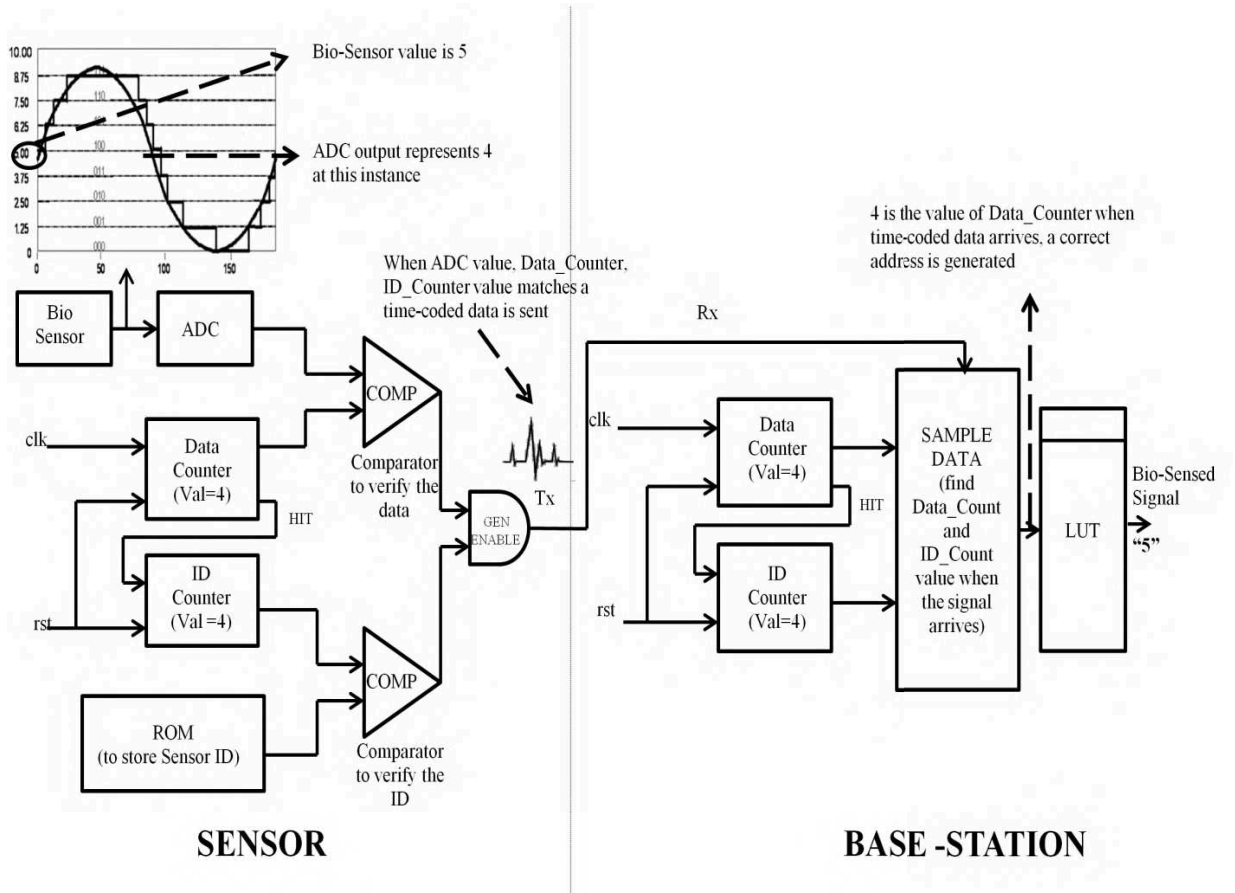
Figure 2.7: Working of TBCD protocol

2.3.2 Comparison with ANT and ZIGBEE

The following calculation is shown to prove the low power consumption of the TBCD protocol. Two state-of-art protocols used in Wireless Sensor Networks, Zigbee and ANT are used for comparison. A comparison study of duty cycles for TBCD, ANT and Zigbee protocol has already been studied and reported in [20]. For an ideal case (where one bit is used to represent the time coded data), the gain in duty cycle of TBCD protocol when compared to Zigbee and ANT protocol is 391 and 234 respectively [20].

22

To study the battery life time of the three protocols, the following three transceivers CC1000 (OOK), CC2420 (Zigbee), nRF24AP2 (ANT) were chosen to find transmit (Tx) power [4, 5, 9]. The life time of the battery in sensor node can be calculated using the formula:

$$Lifetime of battery = \frac{Energy of the Battery}{Active Duty Cycle * TX power}$$

Table 2.6: Battery Life-time for three protocol using its own Transceiver Design

PROTOCOL	DUTY CYCLE [20]	LIFE TIME(in days) (using 20 mAhr/3.3V Battery)	
		0 dBm	∼ -5 dBm
TBCD	0.00032 %	2504	2926
Zigbee	1.25 %	4	5
ANT	0.75 %	7	9

Table 2.6 shows Life time of Battery (using 20 mAhr /3.3V Battery) for three different protocols. Here TBCD is considered to be working in a typical case where 8 bits (including start bit and stop bit) are considered to represent the time-coded data. Table 2.6 proves that TBCD protocol shows the efficiency in prolonging the sensor life time based on small duty cycle in transceiver activity in body. This provides the motivation for enhancing the TBCD protocol to work efficiently in BANs.

2.3.3 Delay calculation of TBCD protocol

This section explains the methodology proposed in [21] to calculate the air delay due to wireless transmission. This method would automatically detect and eliminates any error due to the delay problems. Each sensor node in the network will have different transmission delays. The main theme of protocol is dependent on time-coded data and is necessary to find the correct delay value to eliminate any significant

error in reading the time-coded data.

Initially, it is assumed that all the sensor nodes and the base-station in the network are synchronized. The air-delay between the base-station and each sensor node will be calculated separately with this delay-calculation method. The associated delay with each sensor is found by passing a simple message between base-station and sensor node and will be assigned to its sensor ID stored in a LUT in the base-station.

The delay calculation method was proved using an implemented design in a single FPGA with wireless transceivers for the base-station and each sensor node around it. The base-station sends a signal to each individual sensor and will wait for an immediate reply from each sensor node, but one at a time. The time $(t_2 - t_1)$ represents the delay from the base-station to the sensor node $D(BS\_to\_Sensor)$ and the time $(t_3 - t_2)$ represents the delay from the sensor to the base-station $D(Sensor\_to\_BS)$.

The Fig 2.8 illustrates the working of the delay calculation algorithm. The base-station sends a short signal and starts its counter and waits for an acknowledgement from a particular sensor node. The sensor node after receiving the alert signal $(t_2 - t_1)$ sends an acknowledgement to the base-station immediately $(t_3 - t_2)$. The base-station receives the acknowledgement signal and stops the counter. The total delay would be the sum of the two time periods $(t_2 - t_1)$ and $(t_3 - t_2)$ and is represented by $D(Two\text{-}way)$. The total delay when divided by two will give the delay in one-direction.

The algorithm as provided by [21] is shown here

$D(Two\text{-}way) = (t_2 - t_1) + (t_3 - t_2)$

if $(t_2 - t_1) = (t_3 - t_2)$ then

$D(One\text{-}way) = (t_3 - t_1)$ 2

if $(t_2 - t_1)) \ (t_3 - t_2)$ then

$D(BS\_to\_Sensor) = D(Two\text{-}way)$ - $D(Sensor\_to\_BS)$

More details on Delay calculation for TBCD protocol is reported in [21].
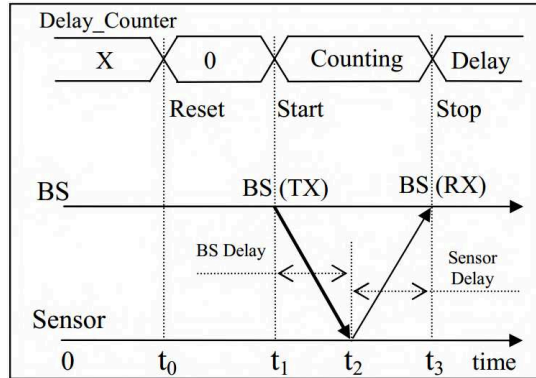
Figure 2.8: Delay Calculation for TBCD protocol [21]

Chapter 3

Clock Drift and Error Compensation

This chapter focusses on clock drift and error compensation methods in TBCD protocol. Section 3.1 gives a brief introduction to clock drift and explains how it affects the synchronisation in TBCD protocol. Section 3.2 discusses about the previous synchronisation cost and similar synchronisation algorithm and its disadvantages. Section 3.3 gives the proposed methodology for delay and drift calculation for each sensor and the error compensation in base station side.

Clock synchronization is an important procedure through which sensor nodes stay intact with a common notion of time and helps in performing a number of fundamental operations in a distributed system. One of the widely used areas of synchronization technique is wireless sensor network. Many protocols of WSN are based on scheduling as it consumes less power than other techniques. For example, Time Division multiplexing, one of the popular scheduling based schemes is applicable only when all nodes of the sensor network are synchronized. It is an essential part in protocols involving localization, security and tracking. As seen in previous chapters, energy efficiency is a key design factor for synchronization in WSN. A Synchronized wake-up and sleep time of the sensor nodes helps in reduction of energy

consumption. Thus, designing energy-efficiency clock synchronization has emerged as an important research challenge.

Consider, a single sensor node and a base station from a particular network. Usually, base-station initiates the synchronisation mechanism by sending a time-stamp message. Theoretically, if the sensor node receives the message successfully, it would calculate the offset between the two clocks through round-trip transactions. In a real environment, the transaction is affected by various delays and clock drifts and thus making clock synchronisation, a tedious task.

3.1   Clock drift

Time synchronization is a huge factor in many energy-critical scheduling operations in distributed systems. The clocks in the electronic system do not run at the same frequency continuously over time, as shown in Fig 3.1 and their synchronisation error for different drift values is shown in Fig 3.2. The frequency variation can be either short-lived due to factors like temperature variations or stay for a longer time due to aging. The difference between the desired and actual time period of the clock is usually bounded by two values and are specified in parts per million (PPM). The frequency error due to change in clock speed is called clock skew. Since, change in the frequency changes with the time, the rate of change of frequency defines the clock drift. A sensor node would drift maximum of $\pm$ k ppm for a network cycle with respect to $\pm$ x ppm of its local clock.

As reported in [20], the relation between the clock drift per second and the clock frequency (f) is given by

$$Drift\_max_{(for1MHz)} = \pm xppm \quad eq(3.1)$$

In general,

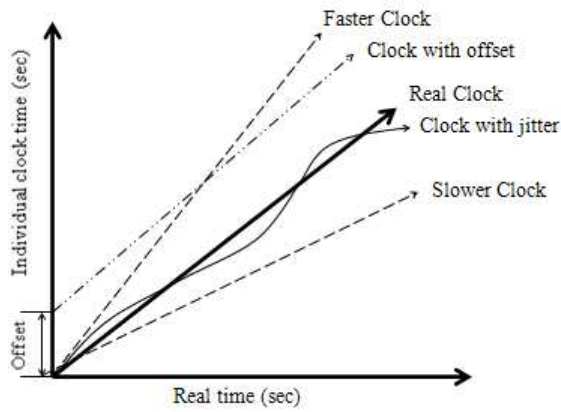$$Drift\_max(fHz) = \pm\frac{(x*f)}{10^6} \quad eq(3.2)$$

27

Figure 3.1: Clocks running at different speeds

From equation 3.1 and equation 3.2 the value of k can be calculated by the given equation

$$k = \pm \frac{(x * f)}{(s * 10^6)} \quad eq(3.3)$$
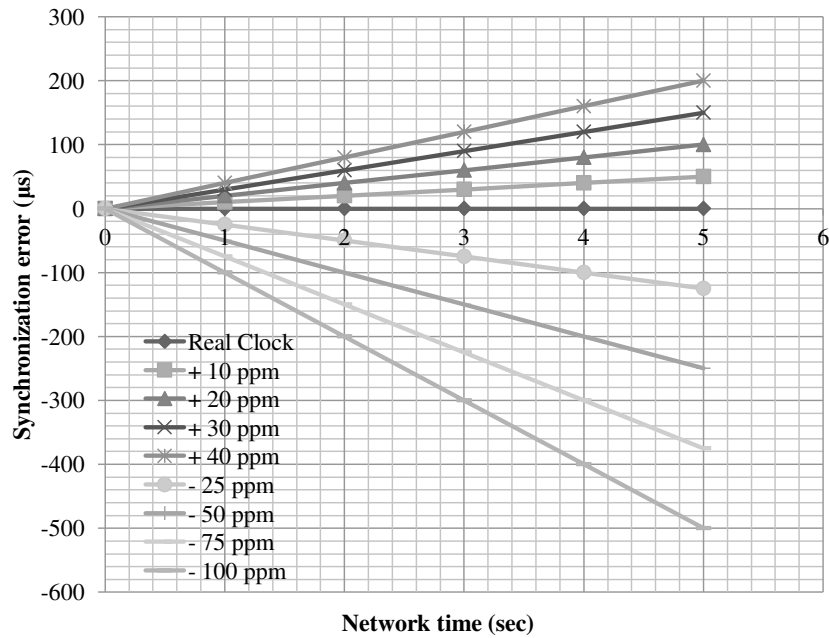
Figure 3.2: Clocks with different drifts

A sensor node running at a local clock with periodic wake-up and sleep times as shown in Fig 3.3, would either wake-up before beacon arrives at A or after the beacon had arrived at B. If the sensor node wakes up at point A, it would receive beacon only after some time. When the drift is positive and the sensor node wakes up at point B, it would miss the beacon message. Both the cases are not good for the network system. In the earlier case, the sensor should loose energy as Synchronisation cost and in the later case, the sensor does miss the synchronization with the base-station. Therefore clock synchronization in WSNs should be designed such that it removes any effects of the random delays in message transactions due to clock drift. To keep all the sensor nodes synchronized within the network, a very efficient and reliable network protocol is needed. Therefore, a series of transaction is required between base-station and sensor nodes to achieve a precise synchronisation. Hence, there is always a trade-off between precise synchronisation and reduced communication energy.
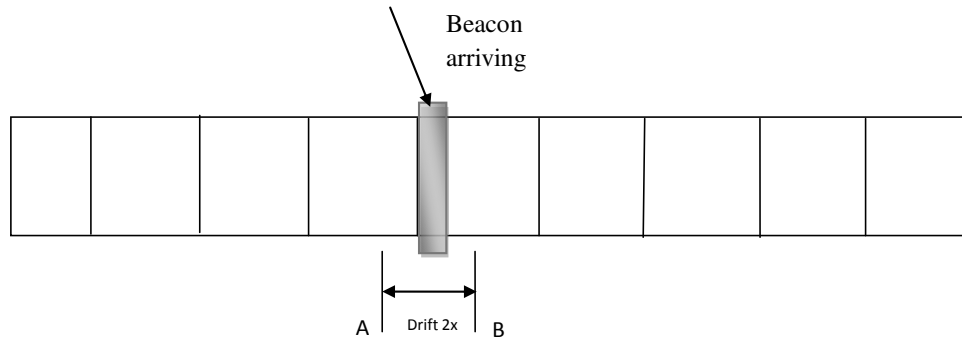
Figure 3.3: Upper and lower bounds of clock drift

Delay calculation method is already provided for TBCD protocol [21]. Even after the delay calculation and error compensation for each sensor node is completed, the sensor nodes gets unsynchronised after certain amount of time. The Table 3.1 shows the time after which different sensor gets unsynchronised after the synchronisation stage is completed.

Table 3.1: Amount of time needed for sensors to get unsynchronised due to clock drift

Sensors	Data Rates (bps)	+ 40 ppm	- 40 ppm
Peak endocardial acceleration (PEA)	10000	2.5 s	2.49 s
Electro-gram (EGM) (μW)	5000	5 s	4.9 s
Accelerometer (G2D)	2000	12.5 s	12.49 s
Bio-impedance (Bio-Z)	1000	25 s	24.49 s

Considering, the relative behavior of one clock y(t) with respect to a real time clock x(t) (i.e.) base-station in case of IWBSNs, the clock y(t) varies with respect to x(t) as reported in [25]

$$y(t) = x(t) + O \quad eq(3.4)$$

where "O" is the Offset between the clocks.

As explained in the previous paragraphs, the drift in a clock is bounded and is specified by a value in ppm (i.e.) Parts Per Million. For example, a clock at 1 MHz rate with +100 ppm will deviate +100 μs in one second. In general, for 1 MHz clock with $\pm$ x ppm indicates a deviation of $\pm$ x μs in one second.

From eq(3.4), the offset between y(t) and x(t) is given by

$$O = y(t) - x(t) \quad eq(3.5)$$

The relative rate of y(t) to x(t) is given by

$$r(t) = \frac{\frac{dy(t)}{dt}}{\frac{dx(t)}{dt}} \quad eq(3.6)$$

The relative drift is the second derivative of r(t) (i.e.) r"(t).

The limitation of the crystal oscillator manufacturer makes the relative drift to increase or decrease within a limit.

30

In [25] it is assumed that there is always a constant x, where $0 \leq x \leq 1$ and the following bounds on the relative drift with x(t) and y(t) is be derived as

$$\frac{2x}{(1+x)} \leq r"(t) \leq \frac{2x}{(1-x)} \quad eq(3.7)$$

So, the protocol for clock synchronization should prevent any error due to the bounded relative clock drift.

3.2   Synchronisation cost

The energy consumed during the time synchronisation service should be very small as possible. When the relative clock drift is estimated from the past synchronization points, it will reduce the communication overhead and also the power consumption. The energy required to transmit one bit is equal to the energy required to execute three million instructions. Hence, energy critical application such as wireless sensor networks requires very small number of transactions for the exchange of synchronization beacons.

An extensive research has already been done on time-synchronization in distributes cases. There are many algorithms for time synchronization such as Asynchronous Diffusion scheme (AD), Network Time Protocol (NTP), Interactive Convergence (CNV) algorithm based on interactive consistency algorithm are all developed for traditional networks. A detailed description of why they are not suitable for low power wireless sensor networks is given in [35, 36, 20].

Reference Broadcasting Synchronization (RBS) is based on Receiver Receiver Synchronization (RRS). The receivers record their local time after receiving the message from the reference broadcast, and then they exchange their recorded time. The offset between any two sensor nodes is measured through exchange of their recorded time. But RBS comes with very high network traffic overhead and leads to very high energy consumption.

Timing Synchronization Protocol (TSP) is based on Sender Receiver Synchronization (SRS) and is very similar to RBS. TPSN is used in symmetric links which is not similar to a body channel. Therefore the algorithm does not fit for IWBSNs. But, it is been widely proved that SRS is better than RBS. Delay Measurement Time Synchronization (DMTS) is a better technique compared to RBS and TSP. The reference node sends a synchronization beacon to all the sensor nodes. The sensor nodes measure the delay by using the time-stamp in the beacon and with their own time. As reported in [20] the synchronization algorithm suffers from high energy consumption, scalability, and computation cost.

Therefore a very low energy protocol is required for time synchronization in case of IWBSNs. TBCD protocol gives a synchronization protocol but did not specify how to estimate the delay including the clock drift. This chapter deals with implementation of TBCD protocol with delay calculation and clock drift.

In the following sections, the implementation of delay calculation and protocol phase are discussed.

3.3 Drift estimation and error compensation

3.3.1 Definitions

To explain the delay calculation, drift calculation and error compensation method, one has to understand the terms 'Network Cycle' and 'Sensor Cycle'. Let us consider, a network with base-station and sensor nodes with n-bit Data_Counter and m-bit ID_Counter.

From Chapter 2 [20], 'Sensor Cycle' is defined as one complete cycle for a sensor node in which the n-bit Data_Counter counts from zero to $2^{(n-1)}$. In this cycle each sensor will send the short signal, whenever the Data_Counter value matches ADC value. 'Network Cycle' is defined as the sum of all the Sensor Cycle or one complete cycle of the network in which the m-bit ID_Counter counts up from zero

to $2^{(m-1)}$ to scan all sensor IDs each once. Using an 'f' Hz clock rate [20]:

$$F = M * N * S$$

If F = f Hz (Clock frequency)

M = 2^m (Total number of sensors)

N = 2^n (Total data steps per sensor cycle)

S = sample/sec (Sample rate)

Then the 'Network Cycle' based on the definition for one sample/sec is [20];

$$Network\ Cycle = 2^m * 2^n = f\ clock\ cycles$$

The scalability of the protocol is clearly reported in [20]. The delay calculation, drift calculation and error compensation is discussed below in both base station and sensor side.

3.3.2 Drift estimation (Base Station)

The different events that occur in base station to calculate the delay and clock drift are discussed below:

- Initially, the sensor node sends T_RST at the start of Network Cycle (i.e.) when Data_Counter and ID_Counter values are zero. The T_RST message is a short message which is spitted into two. The first part contains the node number and second part indicates Sensor_ID for which the synchronisation is done.
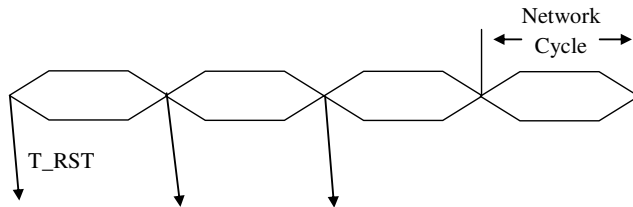

Figure 3.4: T_RST message at the start of Network Cycle

Fig 3.4 shows the base station sending T_RST message at the start of every network cycle.

- Meanwhile, there is another counter called Delay_ Counter which counts during the entire length of the Network Cycle and resets at the start of every Network Cycle. When the Base station gets response from a sensor node in the form of Acknowledgement message #1 (ACK_ 1), Delay_Counter stops and the resultant value gives twice the propagation delay between base-station and sensor node. There are two important events to be noted are (i) by the end of this Network Cycle, the sensor node would have accumulated some offset with the base station in addition to the propagation delay. (ii) The speed of the signal propagation in air is equivalent to speed of light and hence it is assumed that ACK_ 1 will arrive to base station within on the same network cycle. Hence the Delay_ Counter resets at the start of every network cycle. This scenario is shown in Fig 3.5 below.
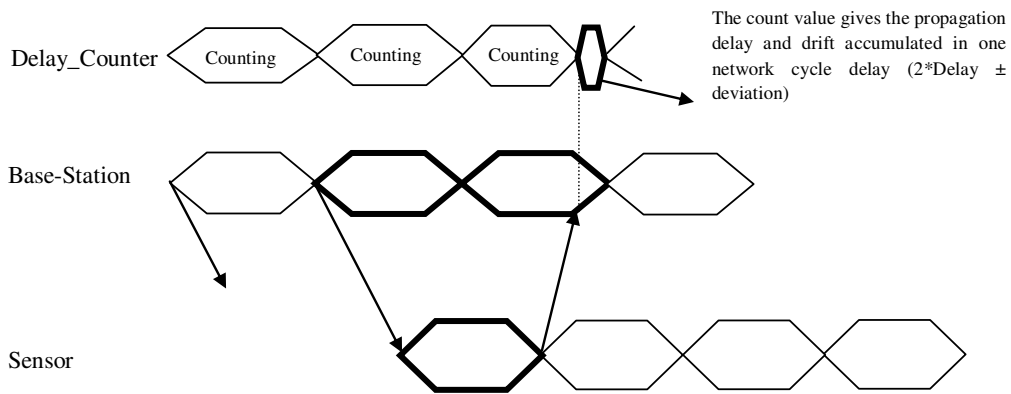
Figure 3.5: Propagation delay for ACK_ 1

- At the start of the next Network Cycle, the Delay_ Counter starts counting from zero. The base station waits for the Acknowledgement message #2 (ACK_ 2). When ACK_ 2 arrives, the Delay_ Counter stops and the value

at which the counter stops represent twice the propagation delay and the drift accumulated over two network cycles.The event is shown in the Fig 3.6.
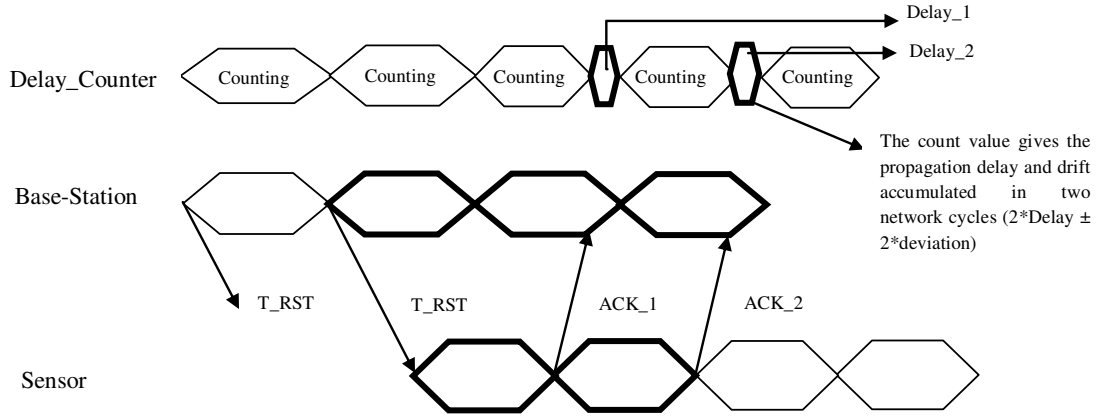
Figure 3.6: Propagation delay for ACK_ 2

- In the next state, the delay and deviation are calculated and stored in a RAM in an address representing the sensor ID. Since Delay_ 1 and Delay_ 2 are given by

$$Delay\_1 = (2 \ * \ Propagation\_ delay) \pm$$
$$(error\ accumulated\ through\ one\ network\ cycle)$$

$$Delay\_2 = (2 \ * \ Propagation\_ delay) \pm$$
$$(2 \ * \ error\ accumulated\ through\ one\ networkcycle)$$

The error due to drift for each sensor is calculated as follows:

$$Deviation\ error = Delay\_ 2 - Delay\_ 1$$

$$Propagation\ delay = Delay\_ 1 - Deviation\ error$$

- The base-station sends an ACK signal to sensor node with the deviation error, implying the sensor node has been synchronised to the network. The base-station continues the same process for the unsynchronised sensor nodes. It then checks whether all the sensor nodes assigned to the network are synchronised.

Figure 3.7: Complete protocol for delay and drift calculation

- When all the sensor nodes are synchronised to the network, the protocol phase starts.

Figure 3.8: State Diagram for base station

36

The whole process is summarised in state diagram in Fig 3.8 and state table in Table 3.2 for the base-station

Table 3.2: State table for Base station

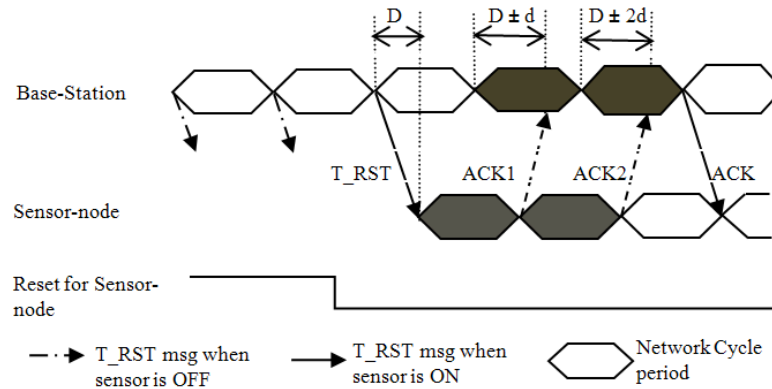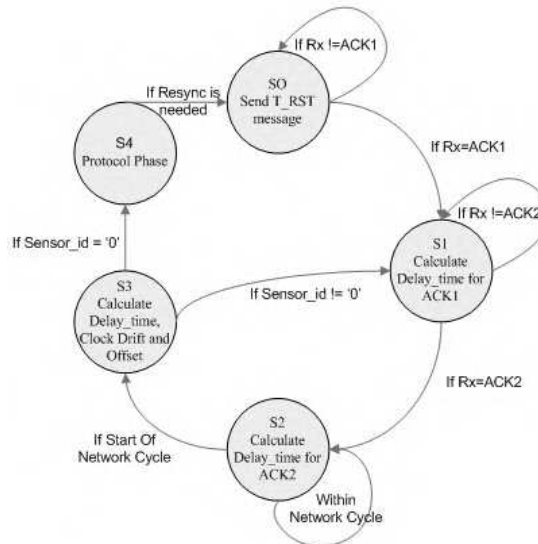| Current State	Condition	Next State	Action
S0	If RX = ACK_1	S1	• Send T_RST message at start of network cycle • Wait for ACK_1
S1	If RX = ACK_2	S2	Calculate Delay_time for ACK_1
S2	If start of Network cycle	S3	Calculate Delay_time for ACK_2
S3	If Sensor_Id = 0 If Sensor_Id ≠ 0	S1 S4	• Calculate Delay_time,Clock_drift • Increment Sensor_ID
S4	If Resynchronisation needed	S0	• Send T_RST message at start of network cycle • Protocol phase

3.3.3 Drift estimation (Sensor Nodes)

The sensor node activities should be minimised due to the energy constraints. The activities of the sensor node were described implicitly in the previous section. Whenever the sensor node receives the T_RST message, it starts its operations. First, the sensor node sends ACK_1 to the base-station which is used to calculate the Delay_1 signal. Then it waits for start of the next network cycle and sends ACK_2 to base station which is used to calculate the propagation delay and deviation. The sensor nodes then waits for the ACK signal from the base-station to ensure it is synchronised to the network.

These are the main events that occur in base station and sensor nodes and high level description is given in state diagram and state table as shown in Fig 3.8

37

and Table 3.3 respectively.
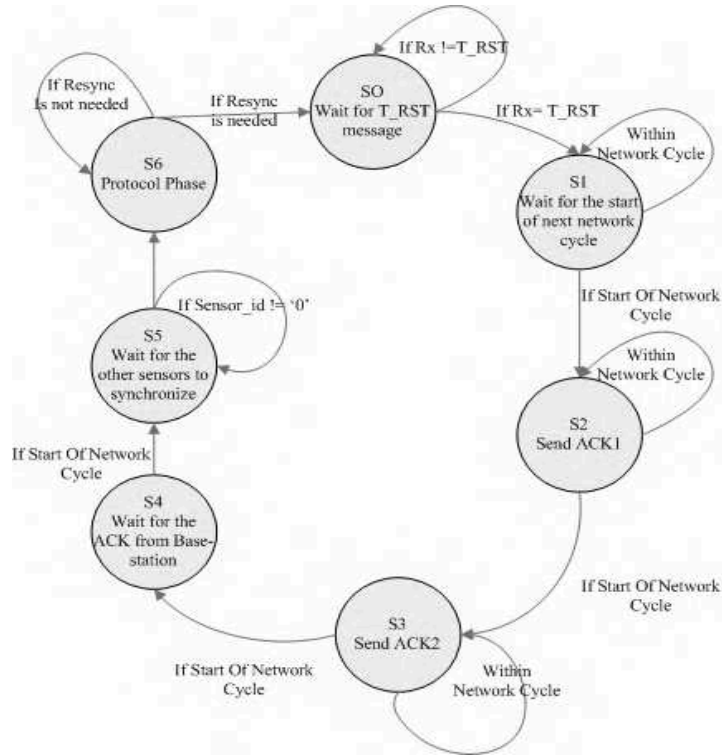
Figure 3.9: State Diagram for sensor node

3.3.4 Error compensation

In the synchronisation phase, the propagation delay for each sensor node is calculated and stored in a Random Access Memory (RAM) in the base-station. The delay values from RAM are later used in the protocol phase, where the compensation for error is done. The control inputs to the RAM are supplied from control block of the base station. It is important to recall that there is a look-up table in the base-station which has all the predetermined values as explained in section 2.3.2. The output to the RAM is given to the block where the correct address to the LUT is generated. The base station remains in synchronisation phase until all the sensors gets synchronised to the network.

Table 3.3: State table for sensor node

Current State	Condition	Next State	Action
S0	If RX = T_RST	S1	Wait for T_RST
S1	If start of Network Cycle	S2	Wait for start of Network Cycle
S2	If start of Network Cycle	S3	Send ACK_1
S3	If start of Network Cycle	S4	Send ACK_2
S4	If start of Network Cycle	S5	Wait for start Network Cycle
S5	Wait for protocol phase	S6	Wait for other sensors to get synchronized
S6	If Resynchronization is needed	S0	Protocol phase

During the protocol phase, the base-station starts receiving the short signal (i.e.) the time-coded data during the time slot allocated for different sensors. An address is generated using the present Data_ Counter and ID_ Counter value, when the short signal arrives to the base-station. This address is later corrected using the delays stored in the RAM. The corrected address generated is used to retrieve the value of bio-sensed signal using the look-up table. Thus, the delay calculated in synchronisation phase helps to decode the correct sensed value of the bio-sensor, without actually sending the whole data. A higher level description of correcting the errors is shown in the flowchart in Fig 3.10.

The surrounding conditions are accessed frequently. The base-station, then call for re-synchronisation, if many sensor nodes goes out of synchronisation. Hence, the delay and clock drift are calculated once again and stored in RAM.
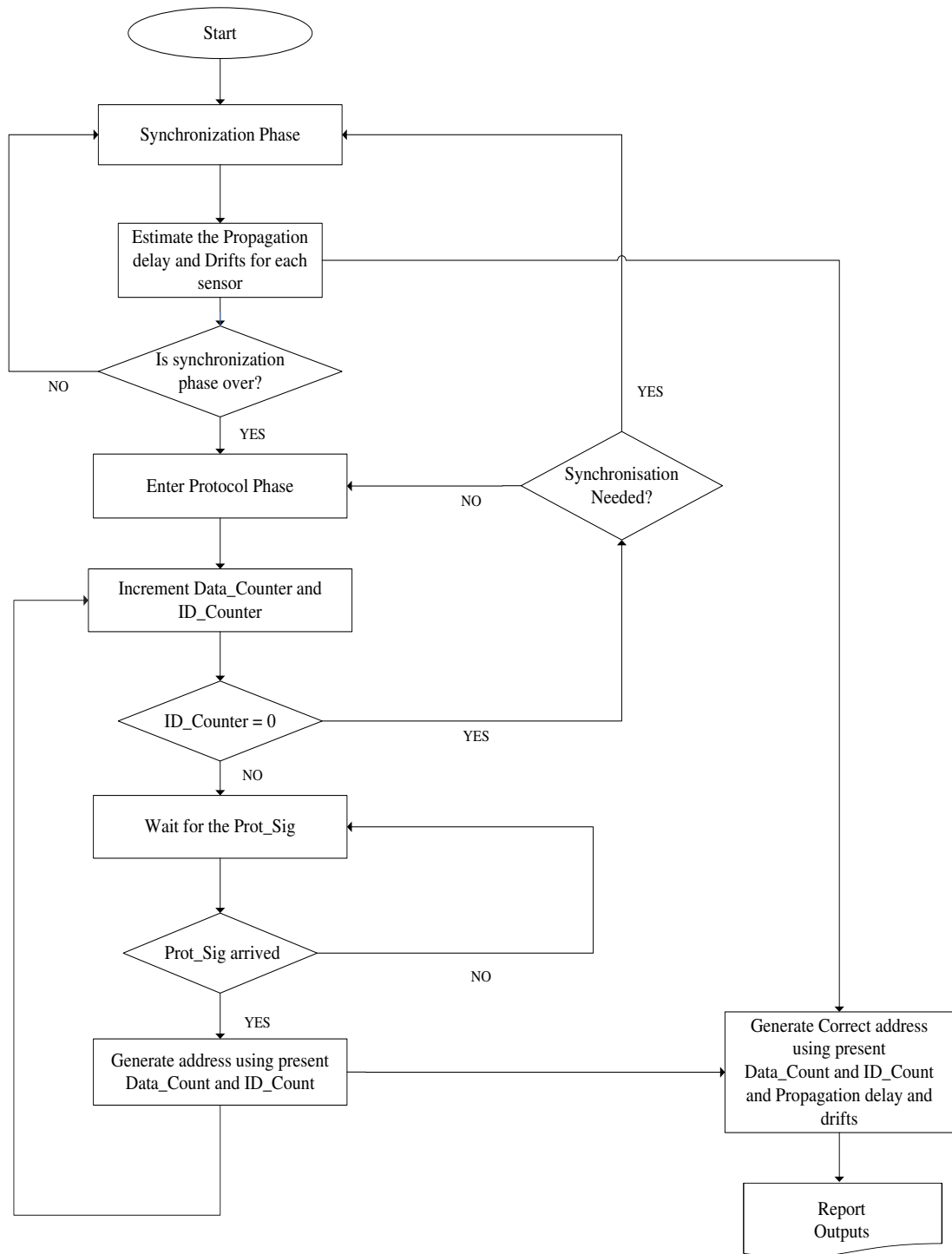
Figure 3.10: Flowchart for error compensation

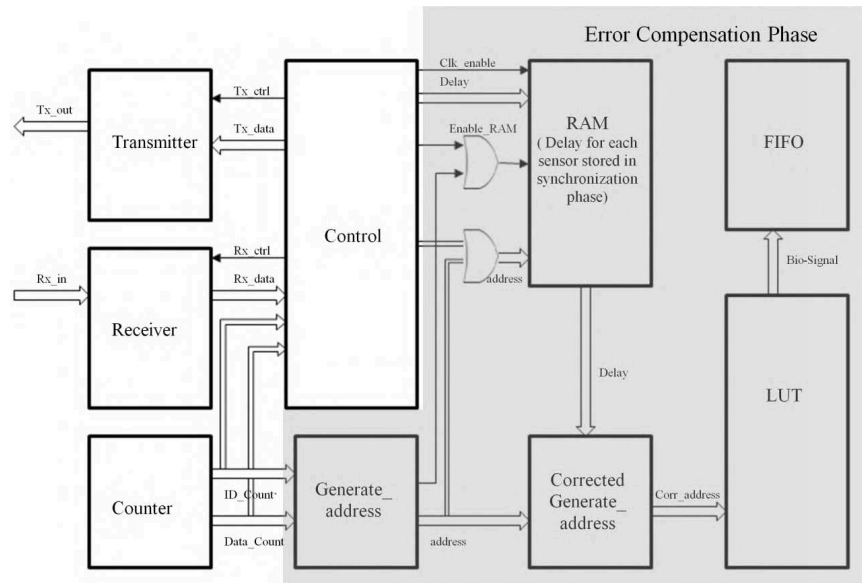### 3.3.5 Model of base station and sensor node

Figure 3.11: Block diagram for base station

The block diagram in Fig 3.11 and Fig 3.12 shows different blocks in the base station and sensor side respectively. The simulation results are provided in Chapter 5.
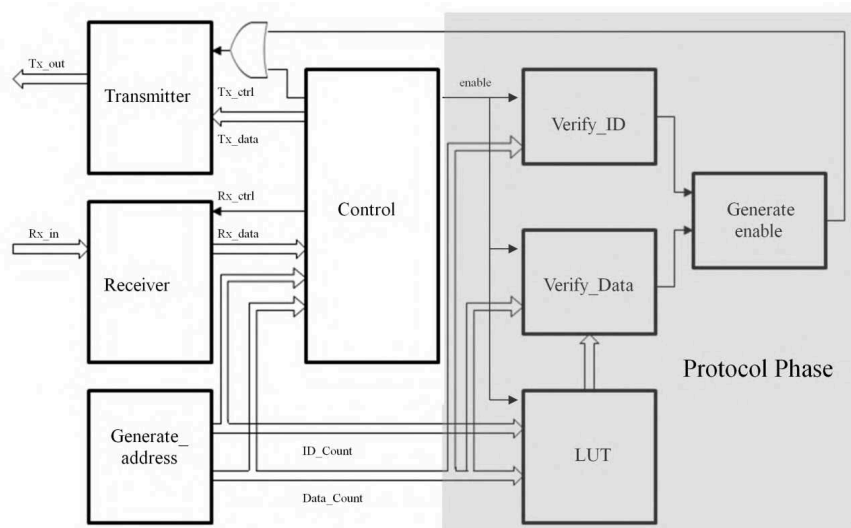
Figure 3.12: Block diagram for sensor node

Chapter 4

Wireless Body Channel

This chapter mainly focusses on the wireless in-body channel. The first section of this chapter provides a brief description about Medical Implant Communication Standard (MICS) and power requirements of implantable body centric communications. The second section explains the characterisation of the body channel. This section provides some basic definitions, brief description of the experiments used by [37] and their results to characterize the wireless body channel. The third section explains the proposed verification methodology for IWBSNs. The final section discusses about the simulation framework, providing details about the modelling of sensor nodes, base-station, wireless body channel and the error compensation phase.

4.1 Body-Centric communication

The communication in and around the human body has been studied to embed health care and multimedia applications. The body centric communication is accepted as an important part of the future mobile communication standards. There is a considerable research taking place to characterize the channel around the body, to produce suitable antennas for the body area networks and to standardize the communication for the implant devices.

The range of body centric communication requirements can be classified as [23]

- Communication between off-body and on-body devices : **off-body**

- Communication between on-body and wearable-body devices : **on-body**

- Communication between in-body and body networks : **in-body**
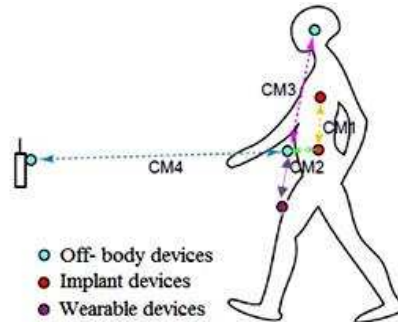
Figure 4.1: Scenarios of Body Centric Communication

The Fig 4.1 shows different type of possible communication in body centric communications. A lot of research works were focused to characterize on-body to off-body communications. Only very few works were attempted on in-body communications due to the difficulty in the measurements inside a living human body. In this work, the focus is given to implantable sensor network communication.

4.1.1 Standards for Medical Implant Communications

Federal Communication Commission (FCC) established Medical Implant Communications standard (MICS) and allocated frequency spectrum of 402-405 MHz to operate implant medical devices. In 2009, FCC revamped Medical Device Radio Communication services (MedRadio) in 401-406 MHz range. FCC added spectrum ranging from 401-402 MHz and 405-406 MHz to the already existing MICS spectrum to form the latest MedRadio services. A separate network can be used for every individual who is using different bandwidths based on the Table 4.1. Thus, MedRadio

allows individuals, medical device manufacturers and medical practitioners to use implanted medical devices such as cardiac pacemakers, defibrillators, neuromuscular simulators without causing any disruption to other users of electromagnetic radio spectrum. The main reasons for choosing these frequencies spectrum are the worldwide availability, reasonable sized antennae and better propagation for the medical implant devices [6].

Table 4.1: Allowed Frequency range and bandwidth for Medical Implant Communications

Frequency Range	Allowed Bandwidth
401-401.85 MHz	100 KHz
401.85-402 MHz	150 KHz
402-405 MHz	300 KHz
405-406 MHz	100 KHz
413-419 MHz	6 MHz
426-432 MHz	6 MHz
438-444 MHz	6 MHz
451-457 MHz	6 MHz

4.1.2   Power requirements

There is a limitation to the allowable maximum power for implant communication. The maximum allowable power for MICS in USA and Europe are as follows [1]

- European Telecommunications Standards Institute (ETSI): Maximum of 25 μW Effectively Radiated Power (ERP) output power.

- Federal Communications Commission (FCC) & Radio-communication Sector (ITU-R): Maximum of 25 μW Effectively Isotropically Radiated Power (EIRP) output power, which is approximately 2.2 dB lower than the ERP level.

The maximum allowable power specifies the signal strength at the surface of the body. The transmitting power should be higher than the maximum allowable

power to compensate for the loss when it is arriving at the surface of the body. The Table 4.2 sums up the allowed range for MICS implantable communication.

Table 4.2: Typical MICS standards for Medical Implant Communications

PARAMETER	MICS (Typical range)
Data rate	250 Kbps
Transmit Power	25 μW (-16 dBm)
Operating Range	0-2 m

4.2 Characterisation of wireless body channel

The previous section of this chapter discussed about the standards for body centric communications. In the following section, the characterization of the body channel is discussed. The 802.15.4, 4a and other WPAN standards were proved not suitable for the in-body communication [40]. IEEE 802.15 Task Group 6 (TG 6) [1] has been working on project called IEEE P802.15 Working Group for Wireless Personal Area Networks (WPANs) to develop the Body Area Networks (BAN). The researchers studied the propagation of RF waves through the tissues of human body. The document Channel Model for Body Area Network (BAN) presented by TG 6 can be used to evaluate the performance of various protocol proposals for body channel communications. It will enable the engineers to design an optimal physical layer of implantable devices. This would also help to extract a better performance from the energy critical system. The knowledge of RF propagation for the implant devices could be gathered through conducting physical experiments. However in this case, it is extremely difficult [38].

A sophisticated and an improved 3D visualization technique presented in [37] is used to derive a statistical path loss model for the implantable devices. This in-body channel model is used to prove the functionality and evaluate the performance of TBCD protocol.

4.2.1   3D visualization technique

The National Institute of Standards and Technology (NIST) have been doing research to advance measurement science by bringing interactive measurement methods. The block diagram of the experimental set-up is shown above in Fig 4.2. The 3D visualization technique is an outcome of their research. The experimental setup contains four main components [37]:
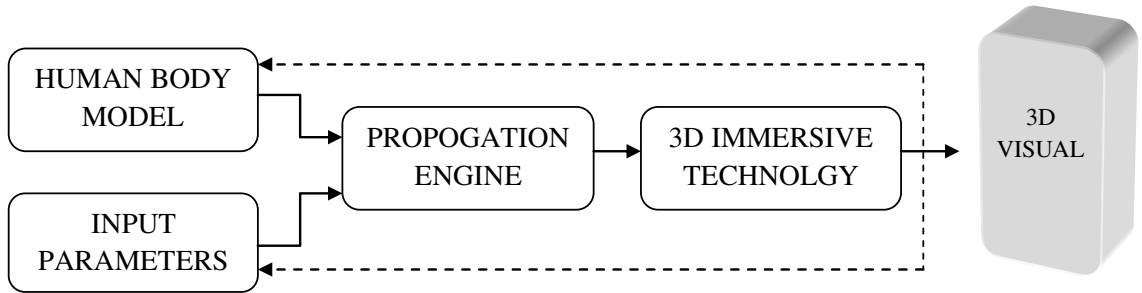
Figure 4.2: Experimental set-up for Body Centric Communication

- Input human body model: It is a 3D human model and has frequency dependent dielectric properties of more than 300 parts of human male body. The properties are the input to the setup and could be changed as desired.

- 3D full wave electromagnetic field simulator (HFSS): It is developed by Ansoft Corporation. It helps in computing different electromagnetic quantities like electric, magnetic field strengths and Specific Absorption Rate (SAR).

- 3D immersive platform: Immersive visualization provides a sense of being physically present in the same space with virtual data representations. The important components in this platform are

    - Three orthogonal screens: It is placed edge-to-edge in a corner of room to provide a 3D stereo scene.

– Motion tracked stereoscope glasses: This allows the user to interact with the 3D object, move and look around it.

– Hand-held motion tracked input device: It is a three button motion tracking device and comes with a joystick. This allows the user to control the elements of the object with a variety of user friendly interaction techniques.

The characterization of wireless body channel using the above mentioned setup is discussed in the following sections. The common input parameters along with the human body model are antennae characteristics, orientation, position and frequency of operation; transmit power, range, resolution and the choice of the output of the system.

One of the important components of the base station and sensor nodes in network is the implant antenna. The environment around which it is functioning is very different from the conventional transceivers. It is very essential to design an efficient antenna for reliable MICS operation and should be isolated electrically from the human body to prevent short circuits. The design should be very small and also bio-compatible. Before that it is important to understand the path loss phenomena.

4.2.2   Path loss

The path loss from a transmitting antenna is defined as the reduction in the strength or density of power of the electromagnetic waves as it travels to the distant receiving antenna. In general, it is defined by

$$PL(d) = \frac{G_r P_t}{P_r d} \qquad eq(4.1)$$

Where PL(d) is the power density loss for a distance d [1]

- G_r is the receiving antenna gain

- $P_r(d)$ is the receiving power at distance d

- P_t is the transmitting power from distance d

In the above eq(4.1), the transmitter antenna gain is included. The body centric communication is not very easy task and the human body is often a hostile environment for wireless signal transmission. The electromagnetic absorption by human tissues, fragmentation of radiation and variations in impedance at the feed reduces the efficiency of transmitting antennae. Therefore, the transmitting antennae gain should be included for MICS communications.

Statistically, for modelling purposes the path loss is given by

$$PL(d) = PL(d_0) + 10 * n * log_{10}(d/d_0) + S \quad d \geq d_0 \qquad eq(4.2)$$

Where PL(d) is the power density loss for a distance d [1]

- 'n' is the path loss exponent which is dependent on the environment in which the electromagnetic wave is propagated.

- 'S' is the shadowing effect. The environmental factors or the movement of body parts will cause change in the path loss from the mean value for a given distance. This phenomenon is called shadowing. It is important to include the shadowing phenomenon for a stationary or non-stationary human body. It represents the deviation value around the mean caused by different body parts and the antenna gain in different directions.

4.2.3   Parameters for the statistical path loss model

The simulations were done with two deep tissue implant devices and four near surface implant devices. The received power was calculated through the simulation for different points. The results were divided into sets of in-body to in-body, in-body to surface, in-body to out-body. For devices near surface loss could occur due

to the clothes and for out-body calculations, free space path loss could be added to get realistic channel model. Fig 4.3 shows the scatter plot of the path loss versus the distance of separation between the transmitter and receiver and also the distribution of shadow fading for deep tissue implant to body surface. The solid line between the scattering points is plotted by fitting a least square regression line. The summary of the experimental results is given in the Table 4.3. The detailed experimental setup and experimental results are given in [37] . The values in the Table 4.3 are used for the channel modelling.

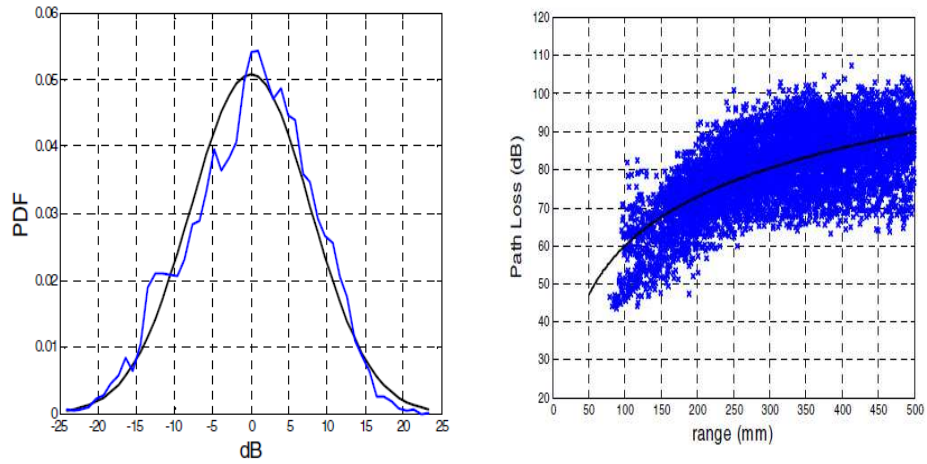Figure 4.3: Distribution of the shadow fading and Scatter plot of the path loss versus distance for deep tissue implant to body surface [37]

Table 4.3: Parameters for the statistical path loss model: (a) Implant to body surface channel [37]

Implant to Body Surface	PL d0(dB)	n	σ_s
Deep Tissue	47.14	4.26	7.85
Near Surface	49.81	4.22	6.81

49

4.3 Verification Framework

The proposed verification framework for wireless body sensor networks is shown in Fig 4.4. Initially, a high level description of TBCD protocol was formed from [19, 21]. As explained in Chapter 3, a modified delay calculation and drift estimation has been added to the protocol which enables the base-station and sensor to stay synchronised for a longer period of time. This modified high level description was used to build the RTL description of sensor nodes and the base-station. The functionality of sensor nodes and the base-station was verified through simulations in Xilinx ISE. It is important to note that the functionality includes synchronisation, error compensation and protocol phases. This was done considering a wired connection between sensor nodes and the base-station. But for any realistic verification, wireless body channel should be considered between sensor nodes and the base-station. The details specified in the previous sections of Chapter 4 is used to provide a realistic environment.

Meanwhile, a high level description of body channel was formed from [1]. This wireless body channel is modelled in Simulink is formed from the high level description. The Simulink model of the transceivers and wireless body channel, RTL description of base-station and sensor nodes were grouped under the Simulink environment. This enables to prove the functionality of TBCD protocol with wireless body channel.

This frame work would enable to evaluate any BAN network protocols in a realistic environment. The synthesized RTL description of base-station and sensor nodes would enable to estimate the power required to carry the MAC logic. The MAC layer could be altered according to the power budget. The simulations would help the designers to estimate the optimum transmit power, receiver sensitivity for the transceivers. The Bit Error Rate (BER) and scorecard analysis helps to evaluate the performance of BAN protocols.

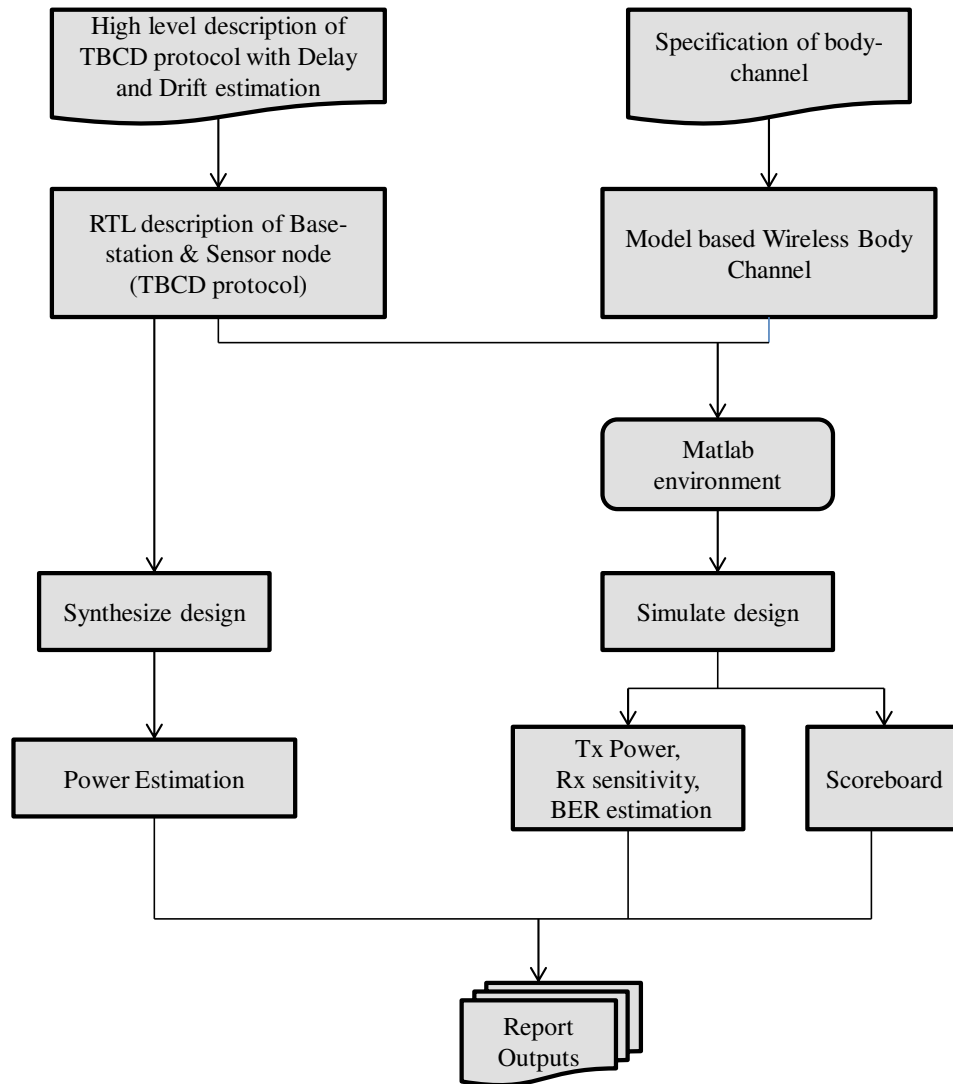Figure 4.4: Verification Framework

4.3.1   Detailed description of simulation environment

The following section discusses how the Table 4.2 is used in the simulation framework which is used in performance analysis of TBCD protocol. The body channel with path loss and shadowing parameters are modeled as specified by IEEE P802.15-08-0780-09-0006 in SIMULINK. The wireless body channel includes the path-loss

and shadowing phenomenon as shown in eq 4.2. The wireless body channel has three important functions: a)Path loss parameters, b)Shadowing, c) dBm to voltage conversion which are converted as a model in Simulink.

The whole communication system framework is done in MATLAB/SIMULINK as shown in the Fig 4.5. The system consists of sensor nodes with OOK modulator, wireless body channel and a base-station with OOK demodulator. In the simulation frame work, eight sensor nodes have been considered and is assumed that all the sensor nodes are synchronised with each other and also the base-station. The data rate follows MICS standard which is 256 Kbps (4 μs). As described in Chapter 2, the time allocated for one sensor node is called "Sensor cycle" and the total time for eight sensor nodes is called "Network cycle". The time for one Senor cycle is (4 μs * 8 (ADC levels)) 32μs. Therefore, the network cycle for the set of eight sensor nodes is (32 μs * 8 sensor cycles) 256μs. The simulations are done for thousand cycles for a range of 50 mm and 500 mm.
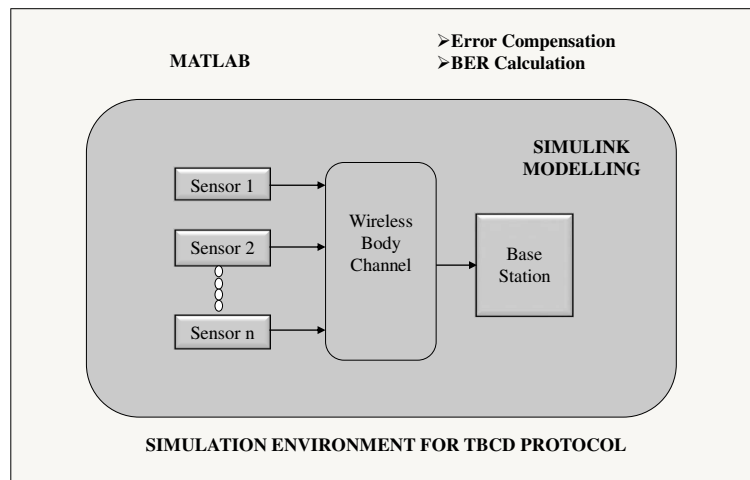

Figure 4.5: Simualtion environment for TBCD protocol

The simulations were done in two phases (i) assuming synchronisation is done (ii) sensors are entering for the first time to network. The blocks of base station and sensor node are shown in the Fig 4.6 and 4.7 respectively were used for simulation

assuming synchronisation is done. For the latter case the models specified in chapter 3 were used. The ID_Counters and Data_Counters are three bits range counters (2^3 combinations).

4.3.2   Sensor node and Base Station
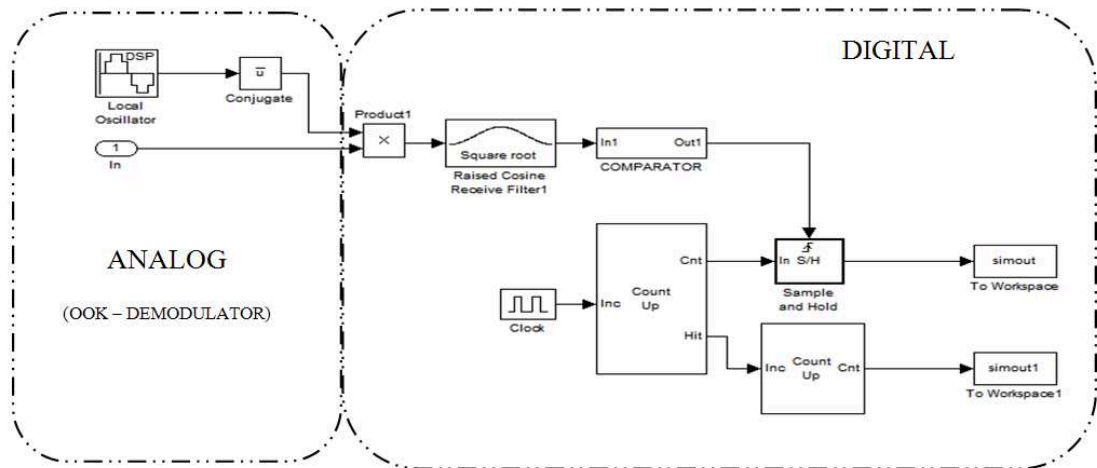
Figure 4.6: Block diagram of Base station

The sensor nodes and base station are designed with wireless OOK transceiver which sends and receives data in the MICS frequency range. There are several trade-offs in using OOK technique such as less-immune to noise, lower spectral efficiency and co-existence. But in the FSK receivers, a Phase-locked loop is necessary and it needs a long-time for start-up which consumes more energy from the battery of the sensor nodes. There are some good techniques proposed to reduce power in FSK. Some special techniques, such as Q-enhanced frontend and sub-harmonic down-conversion were proposed to cut down power consumption, however, they are difficult to implement in multichannel communications and they need more chip area.

Figure 4.7: Block diagram of Sensor node

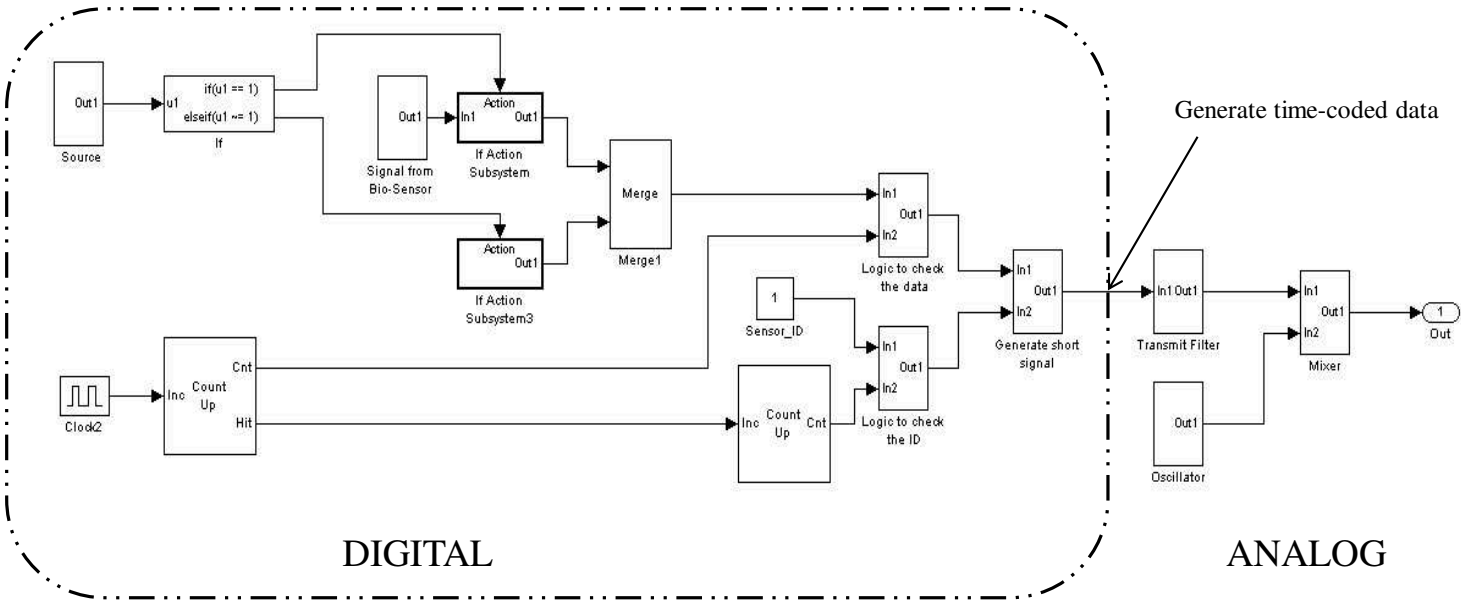Whenever, there is a match between the Data_Counter and ADC value a time-coded data is generated. This short pulse is sent through OOK modulation. The receiver in base station is always ON because it is energy-rich. Once the base-station receives the time-coded data, it decodes the corresponding sensor node number through its ID_Counter, and finds the corresponding sensor data through its Data_Counter and a look-up table.

The frequency spectrum of the simulation is shown in Fig 4.8 below. It shows the signal strength which is -16 dBm at MICS frequency of 403 MHz. The details of the transmit power, receiver sensitivity, the distance between base-station and sensor-node, performance analysis of the protocol are discussed in chapter 5.
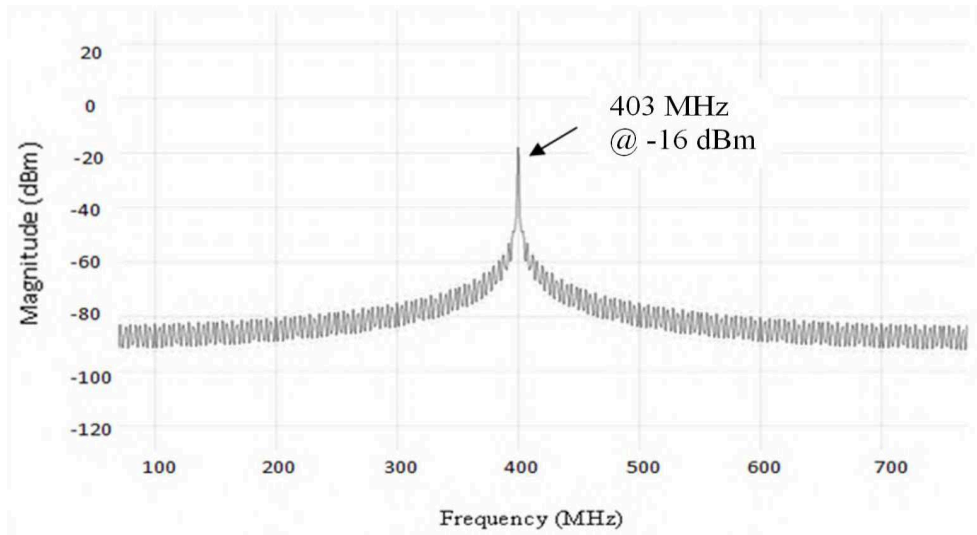
Figure 4.8: Spectrum of MICS signal

4.3.3 Error compensation

The use of calculated delay plays a vital part in base station side. If the delay is more than one clock cycle, the probability is more for the time-coded data to get decoded wrongly in the base-station. This scenario is shown in Fig 4.9. In theory as shown in

Fig 4.9(a), without the effect of delay only one time coded data should be arriving in each sensor cycle. The white circle in Fig 4.9(b) shows two time coded data arriving in the same sensor cycle. The issue is resolved using the delay fixing algorithm which is clearly explained in chapter 3. The scenario for the simulation framework assumes that the base-station and sensor nodes are synchronised. Therefore the simulation results are applicable to the synchronisation phase also.
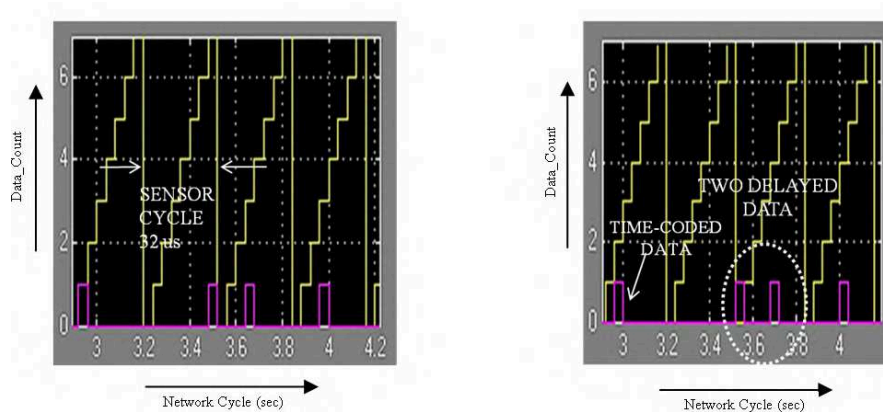
Figure 4.9: Scenario showing two time-coded data arriving in the same network cycle [15]

Chapter 5

Simualtion Results

5.1 Verification of TBCD protocol

In Chapter 3, the modelling of the network components with various clock drifts were shown. This section explains, the simulation results and prove that the protocol works efficiently in real environment. The clocks were made to run at different speeds as shown in Fig.5.1 and the error compensation is explained. The base-station clock is assumed as the ideal clock. The simulations are shown for three phases in the following sub-sections.
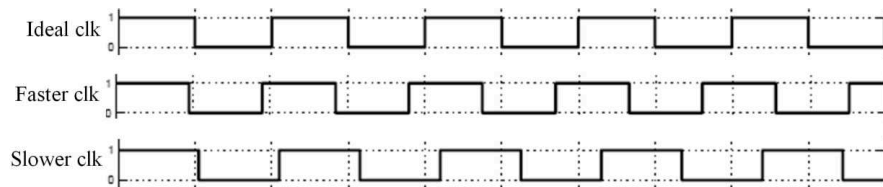
Figure 5.1: Clocks running at different speeds

5.1.1 Synchronisation phase

The first phase shown in Fig 5.2, illustrates the main events of synchronisation between the base station and sensor node.

- Label 1 in Fig.5.2 shows the T‗ RST at the start of Network Cycle (i.e.) when the Data‗ Counter and ID‗ Counter values are zero. The T‗ RST message is a short message which informs the sensor node to start its operation. The sensor is turned ON, and after receiving the T‗ RST message, the sensor node goes to state 1. At state 1, the sensor nodes waits for the next network cycle to send ACK‗ 1.

- The Base station gets response from the sensor node in the form of ACK‗ 1. Label 2 in the Fig 5.2 shows that the counter (count‗ delay‗ 1) has stopped and Delay‗ 1 has been calculated. In state 2, the sensor nodes waits for next network cycle to send ACK‗ 2.

- The Base station gets another response from the sensor node in the form of ACK‗ 2. Label 3 in the Fig 5.2 shows that the counter (count‗ delay‗ 2) has stopped and Delay‗ 2 has been calculated. The value at which the counter stopped (306) represents twice the propagation delay and the drift accumulated over two network cycles.

- Label 4 shows the Acknowledgement from the base station, that the sensor node #1 has been synchronised to the base-station. The clock deviation error (clk‗ dev) is the difference between Delay‗ 1 and Delay ‗ 2.

- Label 5 shows the delay, in terms of the number of data‗ count. '2' represents that the propagation delay between the base station and sensor node requires the same time taken by Data‗ counter to increment twice.

5.1.2   Protocol phase

This phase is already proved in [20] using SIMULINK/MATLAB . The simulations for this phase are provided to show the reader that the base station and sensor node follows three phases as mentioned in TBCD protocol.
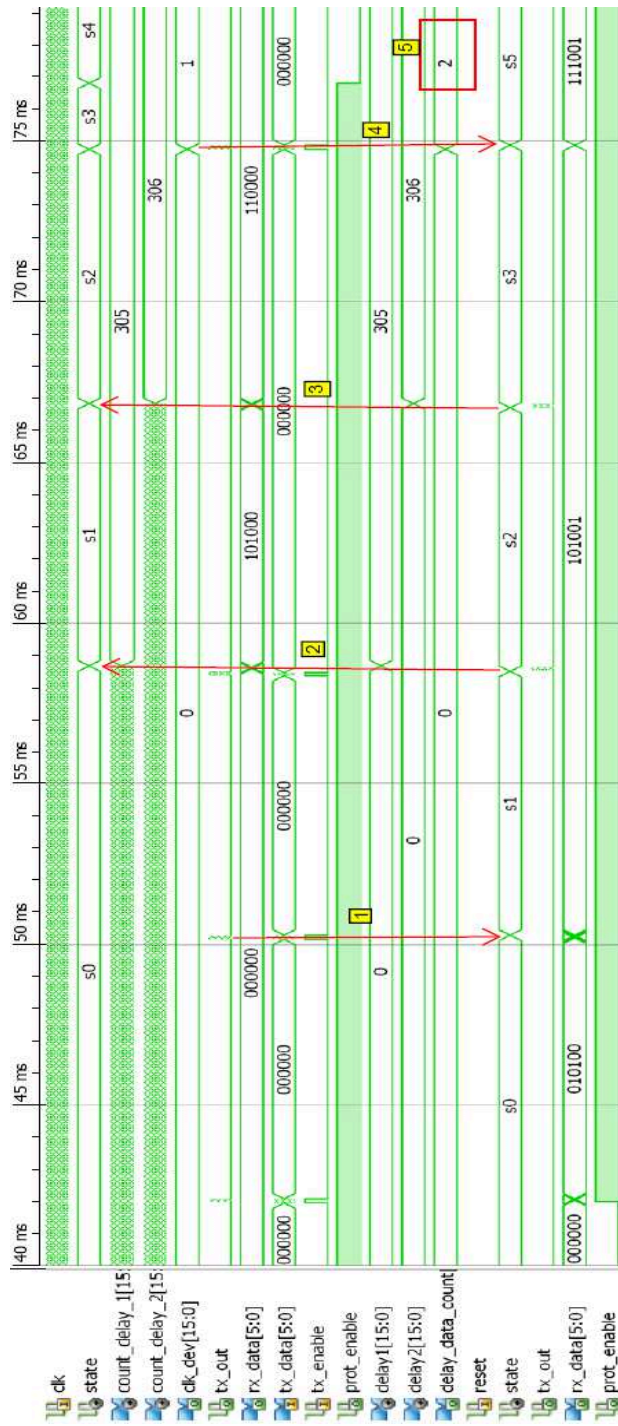
Figure 5.2: Simulations showing Synchronisation phase

59

The second phase shown in Fig 5.3, illustrates the main events between in sensor node in the protocol phase.

- Label 1 in Fig.5.3 shows input signal (data_ in) from the biosensor. The signal from the bio-sensor is in the range [11,12,13,14,15,16,17,18] which is converted to [0,1,2,3,4,5,6,7] by the ADC. For example, Fig.5.3 shows "15 (binary equivalent 1111)", the value being sensed by the sensor. Label 2, shows the converted value by ADC '4' from the look up table. This is represented by the signal data_ out.

- The 'Verify_ Data' block explained in Chapter 3, checks whether Data_ count value and ADC value are equal.The t_ c_ data goes high when there is match in Data_ Counter and ADC value.This scenario is shown in Label 3 of Fig.5.3.

- Meanwhile, the 'Verify_ ID' block explained in Chapter 3, checks for the time slot of sensor node #1.The time_ coded goes high when there is match in ID_ Counter and sensor node #.This scenario is shown in Label 4 of Fig.5.3.

- Label 5 in Fig.5.3 shows the enable signal going high, whenever the t_ c_ data and time_ coded signal goes high. The enable signal is fed to the Transmitter block, which would send the short message to the base station.

The scenario is shown for a single sensor node and base station. In subsequent time slots, the other sensor nodes will go through this phase with same events.

5.1.3   Error compensation phase

In the synchronisation phase, the propagation delay for each sensor node is calculated and stored in a Random Access Memory (RAM) in the base-station. The address generated when the short signal arrives, is altered with the delay stored in the RAM and is used to access the actual value sensed by the particular sensor node.

In this section the error compensation due to clock drift and propagation delay is discussed.

Figure 5.3: Simulations showing Protocol phase

- The base station receives the short signal from each sensors with a propagation delay. The tx_ out signal from the sensor node is transmitted, when enable signal goes high. Label 1 of Fig 5.4 shows the transmitted tx_ out signal due to enable signal discussed in the previous phase.

- Label 2 of Fig 5.4 shows the stored delay for sensor node #1 from the previous phase. Label 3 shows the generated address in the base-station with the ID_ counter and Data_ Counter. The corr_ gen_ add shown in Label 4 is formed by subtracting the delay value with the generated address.

- The enable signal in Label 5 and corr_ gen_ add signal are the inputs to the LUT. The bio_ sensor signal value '15', which was the actual input in the previous phase is correctly decoded even with the propagation delay and the error due to the clock drift. This event is shown in label 6.
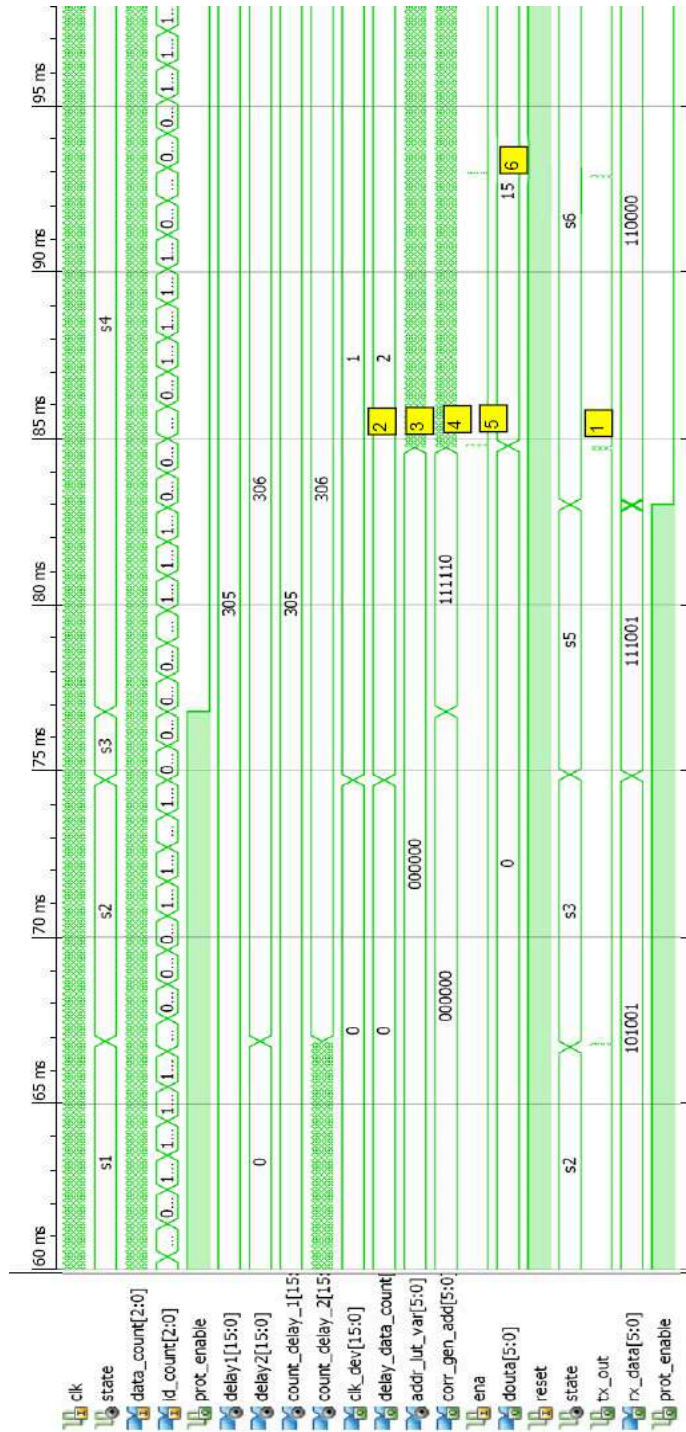
Figure 5.4: Simulations showing Error Compensation phase

62

5.2 Performance analysis
(with wireless body channel)

The experiments were conducted to find the optimum transmit and receive power to compensate for the path loss and to fulfill the Medical Implantable Communication Services (MICS) requirements which is shown in Fig 5.5 and Fig 5.6. The performance of the protocol has been estimated through the Bit Error Rate (BER) versus distance as presented in Fig 5.7 and Fig 5.8.

The deep tissue path loss and shadowing models are added to wireless channel in the simulation framework as prescribed in [1]. The transceivers in the simulation frame work follows MICS standard with carrier frequency of (402-405) MHz and the data rate is 250 kbps.

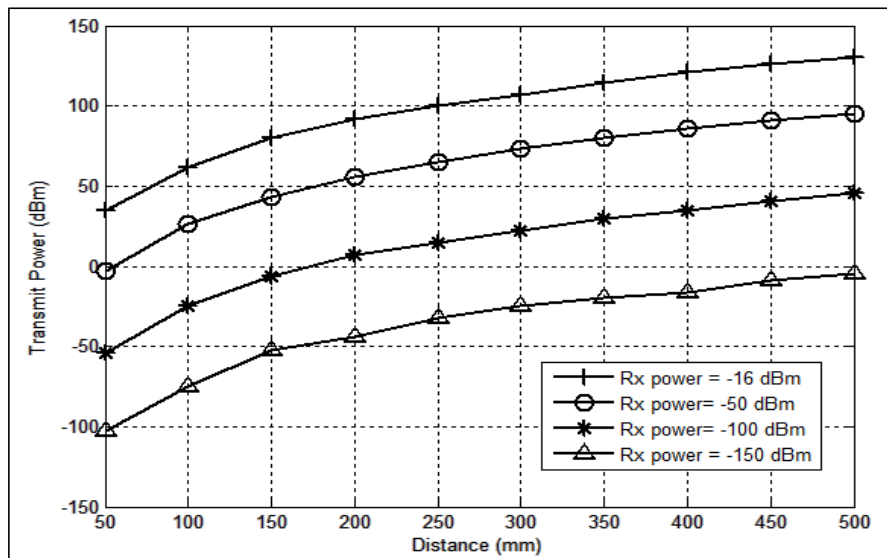Figure 5.5: Required transmit power versus distance inside human body [15]

Since the maximum receive power is -16 dBm at the receiver and recent technologies enable designing transceivers with sensitivity weaker than -100 dBm (eg: CC1000 [4]) and sensitive to very low signals as low as around -150 dBm, simulations were done showing the optimum transmit power to receive a signal strength of -16

dBm, -50 dBm, -100 dBm and -150 dBm at the base-station. The sensor nodes are considered to be placed in ten different locations inside the human body between distances of 50mm to 500mm from the base station. The transmit power has to be increased for longer distances. Fig 5.6 helps to choose sensitivities to design transceivers for different transmit powers.
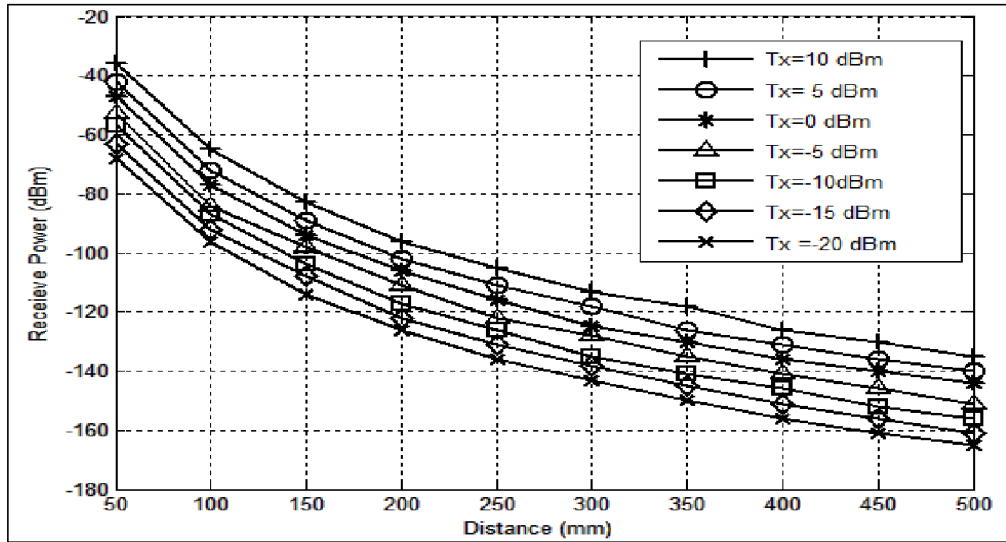
Figure 5.6: Sensitivity versus Transmit power [15]

The BER graphs shows performance of TBCD protocol with the above found optimum transmit power and receiver sensitivity. The EIRP of the transmitters antennae is varied from -25 dBm to 10 dBm. Simulations were done for 1000 sensor cycles. Fig 5.7 and Fig 5.8 show the bit error rate (BER) performance of TBCD protocol against the distance for sensitivity of -125 dBm and -150 dBm respectively. For sensitivity of -125 dBm: erroneous detection in base-station increases from a distance of 30 cm. A higher performance is obtained with lesser sensitivities in the antennae of the base station. From the Fig 5.6 and 5.8, it is clear that, for TBCD protocol to work efficiently for a distance around 50 cm; a receiver sensitivity of -150 dBm is needed.

64

Distance (mm)	100	200	300	400	500
■ Tx Power = 10 dBm	0	0	0.0155	0.34	0.76
■ Tx Power = 0 dBm	0	0	0.244	0.79	0.87
■ Tx Power = -16dBm	0	0.178	0.84	0.87	0.87
■ Tx Power = -25dBm	0	0.611	0.87	0.87	0.87

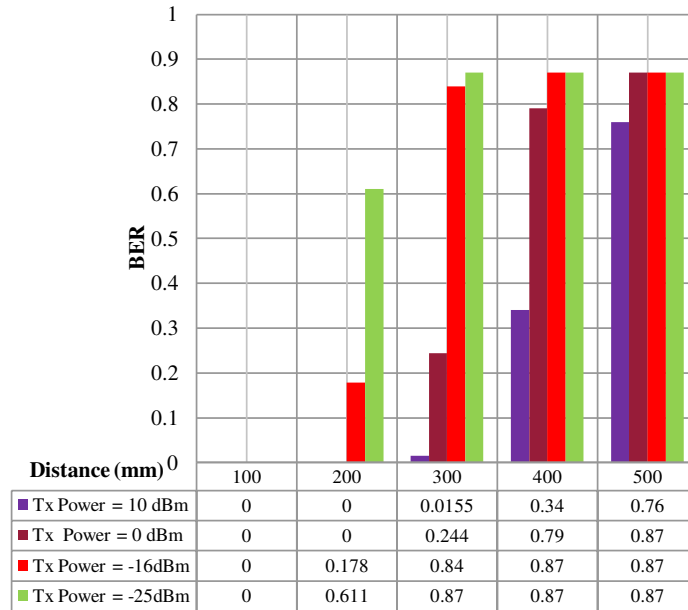Figure 5.7: BER vs Distance between the sensor node antennae and base station antennae (base station receiver is -125 dBm)[15]

It is evident from Fig 5.5 and 5.6 that TBCD protocol can work efficiently for a distance of 50 cm with a transmit power of 0 dBm and sensitivity of -150 dBm. Though -150 dBm sensitivity transceivers are not present now for implantable devices, through the advancements in technology, it will be achieved sooner. But still with suitable error detection techniques we could able to make the network to work efficiently around -100 dBm. The first two curves shown in the Fig 5.5 is impossible for the body area networks as the body cannot withstand such higher powers.

Finally, performance analysis was done including the synchronisation framework. Fig 5.9 shows the number of synchronisation failure and hence would result in the erroneous time-coded-data. This would result in in-correct decoding of bio-signal in the base-station.

Distance (mm)	100	200	300	400	500
Tx Power = 10 dBm	0	0	0	0	0.0073
Tx Power = 0 dBm	0	0	0	0.013	0.177
Tx Power = -16dBm	0	0	0.034	0.459	0.5155
Tx Power = -25dBm	0	0	0.3098	0.7632	0.87

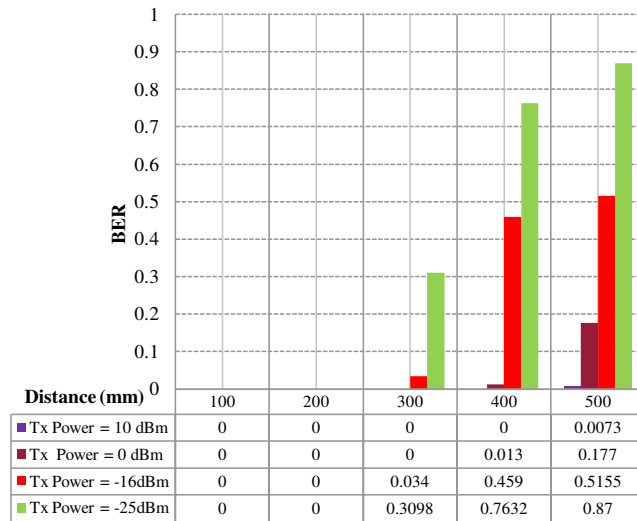Figure 5.8: BER vs Distance between the sensor node antennae and base station antennae (base station receiver is -150 dBm)[15]

Thus, the functionality of the TBCD protocol is proved in section 5.1 and all the figures presented in this chapter sums up the performance analysis of TBCD protocol .
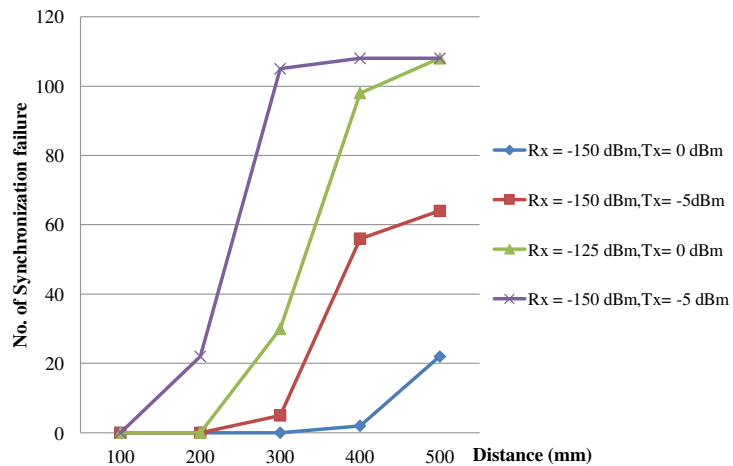

Figure 5.9: Synchronisation failure vs Distance between the sensor node antennae and base station antennae [15]

66

Chapter 6

Conclusion and Future work

The improvements in wireless technology, sensing devices combined with integrated circuits provide a real-time, low-cost health monitoring for the patients [15]. IWBSN needs a very reliable, low-power miniature and fully autonomous architecture that does not disturb the patient's activities. TBCD protocol was formed to provide a very low power sensor nodes. In this thesis, a realistic verification of TBCD protocol was done.

The base-station and the sensor nodes were modeled using HDL and were synthesized using Virtex 5 FPGA. In [21], the clock drift was not taken into consideration. In section 3.1, it is proved that even after synchronisation, the clock drift would make the sensor nodes to go out of synchronisation in a certain amount of time. A drift calculation and error compensation methodology was introduced in the RTL description of sensor node and base-station. The sensor nodes' clocks were made to run with certain drifts to provide a realistic situation. Later, through simulations, the functionality of TBCD protocol in a real environment is proved.

To analyse the performance of TBCD protocol with a realistic body channel, the base station, sensor nodes and body channel are modelled using SIMULINK. This emulates a complete network with an assumption that the synchronisation is done. A verification framework is done in MATLAB. This analysis gives an insight

to the designers about the required transmit power, receiver sensitivity for a reliable communication. A comparison of TBCD protocol was done with the state of art protocols. This thesis proves that the protocol works for a realistic body channel and consumes less energy compared to the state-of-art protocols. The transceivers of TBCD protocol can work up to 7 years versus a few days over Zigbee and ANT protocols.

6.1   Future Work

The body channel is a very high lossy medium and the BAN presents an unpredictable traffic scenarios. Hence, probabilistic analysis of the performance of TBCD protocol could be done as part of future work. A real prototype with all the components of the sensor node could be made and tested on animals for real life environment. Formal verification could be done on TBCD protocol to define the important properties and verify the functionality of the protocol. A low power error correction code suitable for TBCD protocol could be added, to decrease the transmit power and bit error rate.

Bibliography

[1] Bodychannel characeterisation. `http://math.nist.gov/mcsd/savg/papers/15-08-0780-09-0006-tg6-channel-model.pdf`.

[2] Capsil. `http://www.capsil.org/system/files/Chapter+5.pdf`.

[3] Capsil3. `http://www.cs.virginia.edu/~stankovic/psfiles/HCMDSS.pdf`.

[4] Cc1000. `http://www.ti.com/lit/ds/symlink/cc1000.pdf`.

[5] Cc2420. `http://www.ti.com/lit/ds/symlink/cc2420.pdf`.

[6] Fcc , medical radio communiations. `http://www.fcc.gov/encyclopedia/medical-device-radiocommunications-service-medradio`.

[7] Hrcanada. `http://www4.hrsdc.gc.ca/.3ndic.1t.4r@-eng.jsp?iid=33`.

[8] Intel. `http://fiji.eecs.harvard.edu/Mercury`.

[9] Nordic. `http://www.nordicsemi.com/eng/Products/ANT/nRF24AP2-8CH`.

[10] Science daily heart. `http://www.sciencedaily.com/releases/2012/04/120413145305.htm`.

[11] M.A. Ameen, J. Liu, S. Ullah, and Kyung Sup Kwak. A power efficient mac protocol for implant device communication in wireless body area networks. In *Consumer Communications and Networking Conference (CCNC), 2011 IEEE*, pages 1155 –1160, jan. 2011.

[12] Anja Boisen and Thomas Thundat. Design and fabrication of cantilever array biosensors. *Materials Today*, 12(9):32 – 38, 2009.

[13] Zhurong Chen, Chao Hu, Jingsheng Liao, and Shoubin Liu. Protocol architecture for wireless body area network based on nrf24l01. In *Automation and Logistics, 2008. ICAL 2008. IEEE International Conference on*, pages 3050 –3054, sept. 2008.

[14] P. K. Dutta and D. E. Culler. System software techniques for low-power operation in wireless sensor networks. In *Proceedings of the 2005 IEEE/ACM International conference on Computer-aided design*, ICCAD '05, pages 925–932, Washington, DC, USA, 2005. IEEE Computer Society.

[15] S.G. Elangovan, F. Fereydouni-Forouzandeh, and O. Ait-Mohamed. Performance analysis of tbcd protocol over wireless body channel. In *Circuits and Systems (MWSCAS), 2012 IEEE 55th International Midwest Symposium on*, pages 1048 –1051, aug. 2012.

[16] N. Elman, Y. Patta, H.L.H. Duc, K. Daniel, B. Masi, A. Scott, and M. Cima. Micro- and nano-electro mechanical (mems and nems)-based technologies for implanted biomedical devices. In *Electron Devices Meeting, 2008. IEDM 2008. IEEE International*, pages 1 –4, dec. 2008.

[17] Gengfa Fang and E. Dutkiewicz. Bodymac: Energy efficient tdma-based mac protocol for wireless body area networks. In *Communications and Information Technology, 2009. ISCIT 2009. 9th International Symposium on*, pages 1455 –1459, sept. 2009.

[18] Qiang Fang, Shuenn-Yuh Lee, H. Permana, K. Ghorbani, and I. Cosic. Developing a wireless implantable body sensor network in mics band. *Information Technology in Biomedicine, IEEE Transactions on*, 15(4):567 –576, july 2011.

[19] F. Fereydouni Forouzandeh, O. Ait Mohamed, M. Sawan, and F. Awwad. Tbcd-tdm: Novel ultra-low energy protocol for implantable wireless body sensor networks. In *Global Telecommunications Conference, 2009. GLOBECOM 2009. IEEE*, pages 1 –6, 30 2009-dec. 4 2009.

[20] Fariborz Fereydouni Forouzandeh. Ultra low energy communication protocol for implantable wireless body sensor networks, 2010. 9780494711316; 0464: Computer Engineering; 55589251; Applied sciences; Implantable sensors; 857926263; 2297794861; NR71131; 66569; n/a; English; Copyright ProQuest, UMI Dissertations Publishing 2010; 2010; Fereydouni Forouzandeh, Fariborz; Wireless sensor networks; 2012-07-05; M1: Ph.D.; M3: NR71131.

[21] F.F. Forouzandeh, O.A. Mohamed, M. Sawan, and F. Awwad. Delay calculation and error compensation in tbcd-tdm communication protocol for wireless body sensor networks. In *NEWCAS Conference (NEWCAS), 2010 8th IEEE International*, pages 17 –20, june 2010.

[22] Ashutosh Ghildiyal, Balwant Godara, and Amara Amara. Design of an ultra low power mac for a heterogeneous in-body sensor network. In *BodyNets '11: Proceedings of the 6th International Conference on Body Area Networks*, pages 60–66, ICST, Brussels, Belgium, Belgium, 2011. ICST (Institute for Computer Sciences, Social-Informatics and Telecommunications Engineering).

[23] P. S. Hall and Y. Hao. Antennas and propagation for body centric communications. In *Antennas and Propagation, 2006. EuCAP 2006. First European Conference on*, pages 1 –7, nov. 2006.

[24] M.A. Hanson, H.C. Powell, A.T. Barth, K. Ringgenberg, B.H. Calhoun, J.H. Aylor, and J. Lach. Body area sensor networks: Challenges and opportunities. *Computer*, 42(1):58 –65, jan. 2009.

[25] Li-Ming He. Improved time synchronization in wireless sensor networks. In *Software Engineering, Artificial Intelligences, Networking and Parallel/Distributed Computing, 2009. SNPD '09. 10th ACIS International Conference on*, pages 421 –426, may 2009.

[26] Changle Li, Huan-Bang Li, and Ryuji Kohno. Reservation-based dynamic tdma protocol for medical body area networks. *IEICE Transactions*, 92-B(2):387–395, 2009.

[27] Huaming Li and Jindong Tan. Heartbeat-driven medium-access control for body sensor networks. *Information Technology in Biomedicine, IEEE Transactions on*, 14(1):44 –51, jan. 2010.

[28] B. Lo and Guang-Zhong Yang. Body sensor networks - research challenges and opportunities. In *Antennas and Propagation for Body-Centric Wireless Communications, 2007 IET Seminar on*, pages 26 –32, april 2007.

[29] J. Luprano, J. Sola, S. Dasen, J.M. Koller, and O. Chetelat. Combination of body sensor networks and on-body signal processing algorithms: the practical case of myheart project. In *Wearable and Implantable Body Sensor Networks, 2006. BSN 2006. International Workshop on*, pages 4 pp. –79, april 2006.

[30] S.J. Marinkovic, E.M. Popovici, C. Spagnol, S. Faul, and W.P. Marnane. Energy-efficient low duty cycle mac protocol for wireless body area networks. *Information Technology in Biomedicine, IEEE Transactions on*, 13(6):915 –925, nov. 2009.

[31] P.P. Mercier and A.P. Chandrakasan. A 10mbs etextiles transceiver for body area networks with remote battery power. In *Solid-State Circuits Conference Digest of Technical Papers (ISSCC), 2010 IEEE International*, pages 496 –497, feb. 2010.

[32] P.P. Mercier and A.P. Chandrakasan. A supply-rail-coupled etextiles transceiver for body-area networks. *Solid-State Circuits, IEEE Journal of*, 46(6):1284 – 1295, june 2011.

[33] O.C. Omeni, O. Eljamaly, and A.J. Burdett. Energy efficient medium access protocol for wireless medical body area sensor networks. In *Medical Devices and Biosensors, 2007. ISSS-MDBS 2007. 4th IEEE/EMBS International Summer School and Symposium on*, pages 29 –32, aug. 2007.

[34] Hyunchul Park, Yongdae Kim, Eun Sang Jung, and Sejin Kwon. Implantable hybrid chrome silicide temperature sensor for power mems devices. *Micro Nano Letters, IET*, 6(11):895 –899, nov. 2011.

[35] Rodolfo M. Pussente and Valmir C. Barbosa. An algorithm for clock synchronization with the gradient property in sensor networks. *J. Parallel Distrib. Comput.*, 69(3):261–265, March 2009.

[36] Kay Rmer, Philipp Blum, and Lennart Meier. *Time Synchronization and Calibration in Wireless Sensor Networks*, pages 199–237. John Wiley & Sons, Inc., 2005.

[37] K. Sayrafian-Pour, Wen-Bin Yang, J. Hagedorn, J. Terrill, and K.Y. Yazdandoost. A statistical path loss model for medical implant communication channels. In *Personal, Indoor and Mobile Radio Communications, 2009 IEEE 20th International Symposium on*, pages 2995 –2999, sept. 2009.

[38] Kamran Sayrafian-Pour, Wen-Bin Yang, John G. Hagedorn, Judith E. Terrill, Kamya Yekeh Yazdandoost, and Kiyoshi Hamaguchi. Channel models for medical implant communication. *IJWIN*, pages 105–112, 2010.

[39] Sana Ullah, Bin Shen, S.M. Riazul Islam, Pervez Khan, Shahnaz Saleem, and Kyung Sup Kwak. A study of mac protocols for wbans. *Sensors*, 10(1):128–145, 2009.

[40] Hoi-Jun Yoo and Namjun Cho. Body channel communication for low energy bsn/ban. In *Circuits and Systems, 2008. APCCAS 2008. IEEE Asia Pacific Conference on*, pages 7 –11, 30 2008-dec. 3 2008.